San Jose State University
SJSU ScholarWorks

Master's Theses | Master's Theses and Graduate Research

2007

Microaerobic fermentation of engineered E. coli for the production of biofuels

Hiroko Tsuruta
San Jose State University

Follow this and additional works at: https://scholarworks.sjsu.edu/etd_theses

Recommended Citation
Tsuruta, Hiroko, "Microaerobic fermentation of engineered E. coli for the production of biofuels" (2007). *Master's Theses*. 3546.
DOI: https://doi.org/10.31979/etd.99jk-smag
https://scholarworks.sjsu.edu/etd_theses/3546

This Thesis is brought to you for free and open access by the Master's Theses and Graduate Research at SJSU ScholarWorks. It has been accepted for inclusion in Master's Theses by an authorized administrator of SJSU ScholarWorks. For more information, please contact scholarworks@sjsu.edu.

MICROAEROBIC FERMENTATION OF ENGINEERED *E. COLI* FOR THE PRODUCTION OF BIOFUELS

A Thesis

Presented to

The Faculty of the Department of Chemical and Materials Engineering

San Jose State University

In Partial Fulfillment

of the Requirements for the Degree

Master of Science

by

Hiroko Tsuruta

December 2007

UMI Number: 1452046

Copyright 2007 by
Tsuruta, Hiroko

All rights reserved.

INFORMATION TO USERS

The quality of this reproduction is dependent upon the quality of the copy submitted. Broken or indistinct print, colored or poor quality illustrations and photographs, print bleed-through, substandard margins, and improper alignment can adversely affect reproduction.

In the unlikely event that the author did not send a complete manuscript and there are missing pages, these will be noted. Also, if unauthorized copyright material had to be removed, a note will indicate the deletion.

UMI®

UMI Microform 1452046
Copyright 2008 by ProQuest LLC.
All rights reserved. This microform edition is protected against unauthorized copying under Title 17, United States Code.

ProQuest LLC
789 E. Eisenhower Parkway
PO Box 1346
Ann Arbor, MI 48106-1346

© 2007
Hiroko Tsuruta

ALL RIGHTS RESERVED

APPROVED FOR THE DEPARTMENT OF CHEMICAL AND MATERIALS ENGINEERING

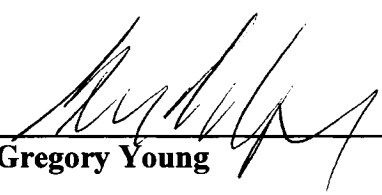

Dr. Gregory Young

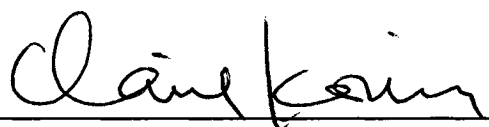

Dr. Claire Komives

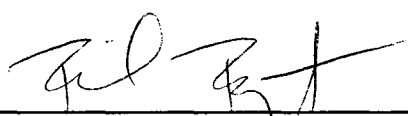

Rika Regentin, Amyris, Inc.

APPROVED FOR THE UNIVERSITY

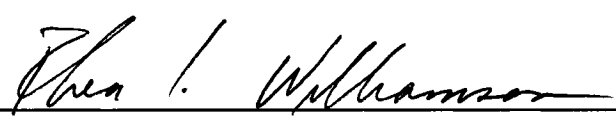

ABSTRACT
MICROAEROBIC FERMENTATION OF ENGINEERED *E. COLI* FOR THE PRODUCTION OF BIOFUELS

by Hiroko Tsuruta

Aerobic, microaerobic, and anaerobic batch cultivation of *E. coli* for heterologous production of mevalonate were performed in bench-scale bioreactors. To screen different degrees of microaerobicity, airflow was kept constant and the amount of oxygen fed into the bioreactor was varied by changing the percentage of air in a gas mixture. Glucose consumption, cell growth, mevalonate, and organic acids were measured and used to determine the yield of mevalonate on glucose. The study showed different distributions of carbon into products. Under aerobic cultivation, the majority of glucose was converted into biomass and CO_2. Anaerobic cultivation made a small amount of mevalonate but primarily produced organic acids and ethanol. At low microaerobic range, glucose was converted into organic acids which accumulate due to the lack of an electron acceptor. At high microaerobic range, organic acids made from glucose were further metabolized to form additional mevalonate and yielded the highest conversion of mevalonate from glucose.

To Rika Regentin, Valerie Foo, and Rupert Yip

For their support, guidance, and encouragement

TABLE OF CONTENTS

LIST OF FIGURES

LIST OF TABLES

LIST OF EQUATIONS

CHAPTER ONE
INTRODUCTION

Biofuels are materials derived from biomass, recently living organisms, or their metabolic byproducts, that can be used as fuels to release energy [1]. Unlike petroleum or coal, biofuels are renewable. Therefore, their production and use as an energy source does not depend on or threaten scarce natural resources. The market for petroleum products was estimated at 1.2 trillion gallons per year in 2003 [2] and this market only grows larger, at the expense of limited resources. An investment in biofuels could provide better energy security, preserve non-renewable resources, and generate steady income to farmers who grow raw materials used in biofuel production.

The biofuels market value is estimated at $27 billion per year and 10.3 billion gallons of sales per year worldwide [3], yet it is still expanding quite rapidly. The fastest growth is anticipated in the U.S. with more than 100 bioethanol production sites under operation and more than 30 under construction [3]. The U.S. biofuels market is driven by rising fossil fuel prices and the phaseout of MTBE in automotive fuels that started in early 2006. In addition, the market has been influenced by government incentives and regulations that support the use of renewable fuels for climate change and fuel security [3].

1.1 Yeast Bioethanol Production

Today's popular transportation biofuel is ethanol. Brazil was the first country to run most of their automobiles on "bioethanol," composed of 85% ethanol and 15% gasoline [4]. Brazilian ethanol is derived from yeast fermentation of sugarcane molasses. A comparable process in the U.S. is the production of ethanol from corn. The

biochemical reactions that take place in yeast fermentation are the result of the glycolysis pathway in central metabolism in Equation 1:

$$1 \text{ glucose} + 2 \text{ AMP} \rightarrow 2 \text{ EtOH} + 2 \text{ ATP} + 2 \text{ CO}_2 \qquad \text{Equation 1}$$

For most microbial cultivation, not ethanol production necessarily, certain parameters are controlled to maintain optimal conditions for the organism to grow and produce the product of interest. These parameters include temperature, pH, dissolved oxygen (DO) concentration, and feed rates. The DO concentration can be maintained by increasing the stir rate and supplying oxygen (i.e., oxygen enrichment) to the fermentor during the cultivation.

In the case of yeast ethanol production, neither pH nor DO concentration is controlled and the process is operated in a non-sterile "open system" [5]. Since the organism can grow at fairly low pH, pH control is not used at industrial scale. In addition, no DO control is necessary since anaerobic or microaerobic processes favor efficient transformation of glucose to ethanol, rather than to cell mass [6]. The cultivation can be done in a non-sterile environment because most contaminants cannot grow at low pH. The organism is also preferred since it can withstand extreme environmental stresses including high osmolality and high ethanol and organic acids concentrations [5]. The yeast ethanol process offers simple reactor design, thus it is suited for the fuel ethanol industry. Ethanol fermentation processes reproducibly deliver 3 g/L/h ethanol productivity and achieve 95% of maximum theoretical yield [5]. Bioethanol is produced at $1.28 per gallon [7] and is sold at $2 per gallon today [3].

Companies such as Novozymes, IoGen, and the National Renewable Energy Laboratory have been investing in the technology to convert waste biomass into bioethanol using genetically engineered bacteria [3]. The corn supply is not sufficient for sustaining long-term ethanol production, thus organisms capable of breaking down cellulose contained in corn fiber and enzymes that can convert cellulosic feedstocks to sugar are the focus of their research.

Although ethanol production is a robust process at scale, it poses challenges as an automotive fuel due to its lower energy density, increase in volatility when blended with gasoline, and miscibility with water [8]. Ethanol provides only 70% of the energy density of gasoline and its tendency to absorb water leads to corrosion inside the engines and storage tanks [8]. Transportation by barge, rail, or truck must be considered instead of using the existing fuel pipelines due to the water miscibility [7].

1.2 Biobutanol

Biobutanol is another research focus in alternative fuels. Its chemical properties are superior to that of ethanol with higher energy content (but lower than gasoline), lower volatility, and low solubility in water. Due to its low volatility, butanol may be used as an oxygenate in some states, eliminating the need for special blends of gasoline during the summer and winter months [7]. Unlike ethanol, butanol transportation can be handled using fuel pipelines. Furthermore, biobutanol can be used to replace gasoline 100% gallon for gallon, while ethanol can only be used at 85% (15% gasoline) [7]. More than a billion gallons of biobutanol are produced per year with an average price of $0.90 per lb in 2007 [9].

The investors in biobutanol are DuPont and British Petroleum. The joint venture expects to produce 10 million gallons per year of biobutanol in a converted ethanol production facility in U.K [3]. DuPont is developing a biobutanol production process using microbial fermentation of sugar beets. *Clostridium beijerinckii* has been selected as a production host [9]. On the downside, toxicity may be a potential concern with butanol. Biobutanol is toxic to the host organism which results in low product concentrations in the bioreactor [9]. Better engineered microbes and processes must be used to overcome the problem [9].

1.3 Metabolic Engineering and Heterologous Production

Metabolic engineering is used to alter biosynthetic pathways to optimize regulatory processes within cells, usually to increase the production of a desired substance [10,11]. The work on metabolic engineering to introduce recombinant genes (non-native genes) into *Escherichia coli* for improved heterologous production has been published since the 1980's. Recently, combinatorial engineering approaches have been developed to improve the production of secondary metabolites in microbial cells [11]. Metabolic pathway genes from multiple organisms are combined to generate novel or improved pathways to biosynthesize products that were previously inaccessible [11]. The application of combinatorial engineering to *E. coli* has improved the production of many products, including polyhydroxyalkanoate (PHA) for biodegradable polymers [12], polyketides for use as antibiotics, and isoprenoids for commercial flavors, fragrances, and therapeutic agents [11].

An advantage to the combinatorial engineering approach is illustrated in the following example. Terpenoids are naturally occurring compounds found mostly in plants that can be of medicinal use. The levels of terpenoids produced by plants are minuscule, thus harvesting plants to extract these molecules for commercial use is expensive. Similarly, total chemical synthesis of these compounds is complex and costly [13]. To overcome these limitations, Martin [13] engineered the production of terpenoids in a microbial host by introducing a non-native mevalonate isoprenoid pathway into *E. coli*. His study showed production of 24 mg/L of amorphadiene, a precursor to an anti-malarial drug [13].

E. coli is often chosen as a host to function as cell factories to mass produce these commodity chemicals. The advantages of using *E. coli* include easy, well established genetic tools, rapid robust growth, and simple nutritional requirements [14]. Furthermore, *E. coli* is a well behaved production host for large scale manufacturing [15]. Once the recombinant *E. coli* is constructed, fermentation process development work is undertaken to maximize the specific productivity of the secondary metabolite (g/L/OD (cell mass)/h). The term "fermentation" was traditionally used to refer to anaerobic respiration of the cells converting glucose to acetate, ethanol, or other organic acids; however, it is used more generally today to encompass any microbial bioprocess [6].

1.4 Isoprenoids as Fuel Molecules

While butanol is superior to ethanol as a fuel molecule, it is not the only microbial produced compound with potential as a fuel. Production of isoprenoids by fermentation has been demonstrated for many compounds [16] and this family of molecules includes

some with interesting fuel properties. The key properties required in making good biofuels are high octane number, low vapor pressure, oxidation stability, and water tolerance. Through metabolic/combinatorial engineering around the isoprenoid pathway, one can create a strain that produces a desired fuel molecule (e.g., longer carbon chain, desaturation, branched molecule) with these properties. Once the strain is constructed, the heterologous production of new biofuel molecules can be carried out by microbial fermentation, preferably similar to that of the ethanol production (i.e., simple reactor design) for advantages in scale up and process transfer.

With superior fuel properties, a novel isoprenoid biofuel compound could out-compete ethanol in the biofuels market. Assuming that the cost per gallon of the production of the isoprenoid biofuel compound is comparable to bioethanol production (e.g., same raw materials, same anaerobic process), the novel compound could earn more market share due to higher energy density, higher allowable blend in gasoline, and better fit in existing fuels infrastructure.

1.5 The Mevalonate Pathway

In many organisms isoprenoids are generated from the mevalonate pathway. The pathway is found native to eukaryotes, and is responsible for the production of cholesterol in animal cells and ergosterol in fungi [16]. The pathway can be divided into two parts in yeast *Saccharomyces cerevisiae*: an isoprenoid pathway ending with the formation of FPP (farnesyl diphosphate) followed by a pathway dedicated for ergosterol (e.g., steroids) biosynthesis [16] illustrated in Figure 1. The early steps of the mevalonate pathway are of interest because they generate precursors for the synthesis of isoprenoids.

Martin [13] published studies of heterologous production of terpenoids in a microbial host by introducing mevalonate isoprenoid pathway from *S. cerevisiae* into *E. coli*. Since all terpenoids are derived from the same universal precursors of IPP (isopentenyl diphosphate) and DMAPP (dimethylallyl diphosphate), host microbes engineered to produce a large quantity of these precursors are beneficial for the biosynthesis of any terpene [13].

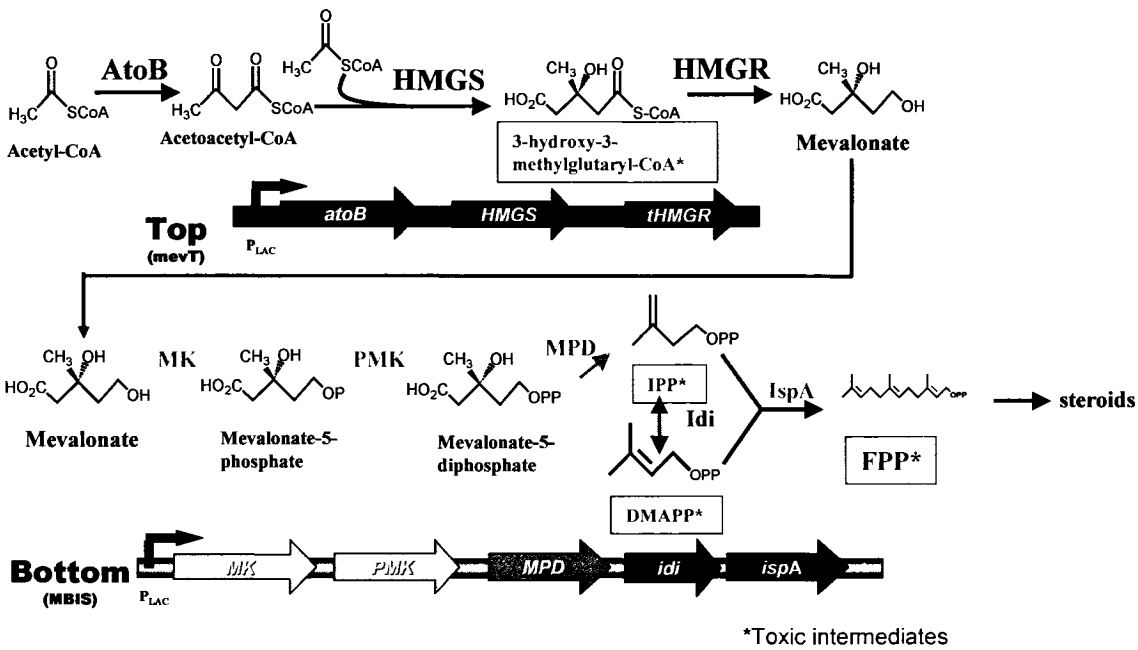

Figure 1. Mevalonate pathway.

CHAPTER TWO
LITERATURE REVIEW

2.1 Aerobic, Anaerobic, and Microaerobic Cultivations and Processes

Most *E. coli* fermentation processes for heterologous production are operated under aerobic conditions. This is because high cell-density aerobic conditions offer fast growth rates [17], high growth yield coefficients ($Y_{x/s}$) [18], and high productivity [19]. Lawford described cell mass yield on sugar substrate as directly proportional to the amount of cellular energy (ATP) generated from the catabolism of that sugar [18], and ATP generation from glucose is much higher in aerobic processes.

Aerobic catabolism of sugar can be divided into three phases as shown in Figure 2: 1) glucose (C_6) is broken down into pyruvate (C_3x2) via glycolysis, followed by 2) conversion of pyruvate to acetyl-CoA, then to CO_2 and NADH in tricarboxylic acid cycle (TCA), and 3) transferring of electron down the electron transport system chain (ETS chain) from NADH to an electron acceptor to initiate the formation of ATP [6]. During glycolysis, the cofactor NAD (i.e., NAD+) is reduced to NADH when it accepts two electrons to oxidize an intermediate substrate into pyruvate (i.e., oxidation-reduction reactions). Similarly, additional NADHs are generated from each cycle of TCA. Under aerobic cultivation, ATP is formed most efficiently with the presence of molecular oxygen as a terminal electron acceptor in the ETS chain [6]; all NADH generated by glycolysis and the TCA cycle are processed through the ETS chain and reoxidized back to NAD, which is required to restart the glucose metabolism. If cells had no means to reoxidize NADH to NAD, a pool of NADH would accumulate and halt further sugar catabolism. Aerobic

processes generate the most ATP (a maximum of 36 ATP per mole of glucose for *E. coli*) and make higher cell mass; hence, aerobic processes are used for high cell density cultivation to achieve high heterologous productivity. However, it is worth noting that high productivity is entirely due to the mass population of cells. When productivity comparisons are normalized by the cell concentrations obtained under the different environmental conditions, the specific productivity is found relatively unaffected by oxygen availability [18].

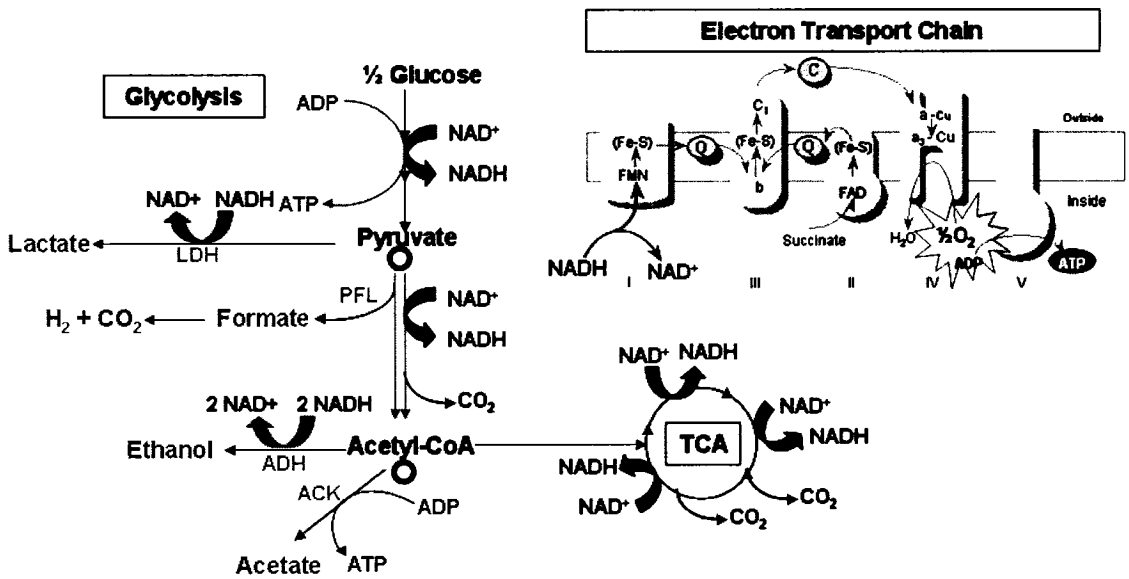

Figure 2. Glucose metabolism via glycolysis, TCA cycle, and ETS chain in *E. coli* [20]. Anaerobic (left) and aerobic (right) routes. Open circles indicate branch points of the respiratory and fermentative catabolism [21].

In contrast to aerobic growth, anaerobic microbial cultivation does not promote fast growth rate and is unable to generate high biomass. This is a major constraint [17] when aiming for high productivity based on cell mass. The typical biomass yield on

glucose of respiratory cultures is reported as 0.5 g per gram of glucose, whereas the yield of anaerobic culture is found to be five-fold lower [22]. Another constraint involves the redox balance. Glycolytic NADH must be reoxidized back to NAD. Under anaerobic conditions, reducing equivalents are transferred to metabolic intermediates rather than the ETS chain since the external electron acceptor O_2 is lacking [21,23]. This results in the synthesis of reduced fermentation products in ratios necessary to generate ATP and reoxidize the NAD(P)H generated by glycolysis to NAD(P) [24]. In *E. coli*, one mole each of ethanol and acetate and two moles of formic acid are produced per mole of glucose under anaerobic, no-growth conditions [24]. This translates to only three moles ATP generated per mole of glucose.

However, there are some advantages in operating microbial cultivation under anaerobic conditions when considering large scale production. Anaerobic processes can be run with simple reactor design, control strategy, and operating conditions since oxygen mass transfer limitation or non-ideal reactor mixing are not an issue [25]. In terms of feedstock nutrients, the carbon (sugar) fed to the microbe is not wasted on generation of CO_2 due to a decline in TCA cycle flux during anaerobic cultivation [26]. Similarly, while aerobic cultivation allows conversion of more carbon substrate into biomass and thus decreases product yield, anaerobic cultivations can convert carbon into products, rather than biomass accumulation, allowing higher yield of product per substrate ($Y_{P/S}$) [27]. The most successful anaerobically produced products are those that cells make in order to generate ATP and regenerate NAD, such as acetate and ethanol [24]. *E. coli* strains which were engineered to exclusively biosynthesize lactate during anaerobic

growth achieved yields of 0.86 g lactate/g glucose [14]. Heterologous pathways that generate ATP or regenerate NAD could best take advantage of anaerobic conditions. In terms of commercialization, however, the biggest advantage in choosing anaerobic process for the heterologous production of biofuel chemicals is that the process would be similar to industrial ethanol production process which is shown to be feasible at a very large scale [28] and the processes would fit into existing facilities without additional capital investment.

Operating conditions between aerobic and strict anaerobic processes are referred to as microaerobic processes. Microaerobicity describes conditions where oxygen is consumed by cells as fast as it is supplied, thus the dissolved oxygen content in the liquid is always close to zero. A measure of dissolved oxygen concentration in the liquid phase is referred as DOC and measured in percent of saturation by a DO probe. A DO probe is calibrated 0% pO_2 with 100% N_2 gas and 100% pO_2 with air. In the presence of microbes in the culture, 0% DOC signifies one of the two situations: 1) N_2 is sparged into a bioreactor and no air (no oxygen) is supplied, or 2) cells are consuming oxygen as fast as it is being supplied. In terms of growth, the DOC close to zero limits the microbial rate of growth in microaerobic processes, thus high cell density culture is not feasible, but better cell growth than a strict anaerobic process is obtained. Also, the redox balance for microaerobic process lies in between that of aerobic and anaerobic processes. For aerobic and anaerobic respirations under steady-state conditions, NADH/NAD ratio of 0.02 and 0.75 was observed, respectively [21]. For microaerobic respirations, only a trace amount of oxygen supply at the level of 0.2 μM DOT (dissolved oxygen tension)

was enough to reduce the ratio significantly to 0.4 as shown in Figure 3 (a). With incremental increases in oxygen supply rate under microaerobic conditions, the NADH/NAD ratio gradually approached the level under fully aerobic conditions [21]. The same fermentation byproducts as the anaerobic process were detected under microaerobic conditions but in lower amounts. Interestingly, the carbon wasted on byproducts such as acetate can be reused by the cells completely with the presence of oxygen [27]. Finding operating conditions within the microaerobic range that support low cell density growth, low redox ratio, and improvement in carbon flux down the heterologous pathway is desirable.

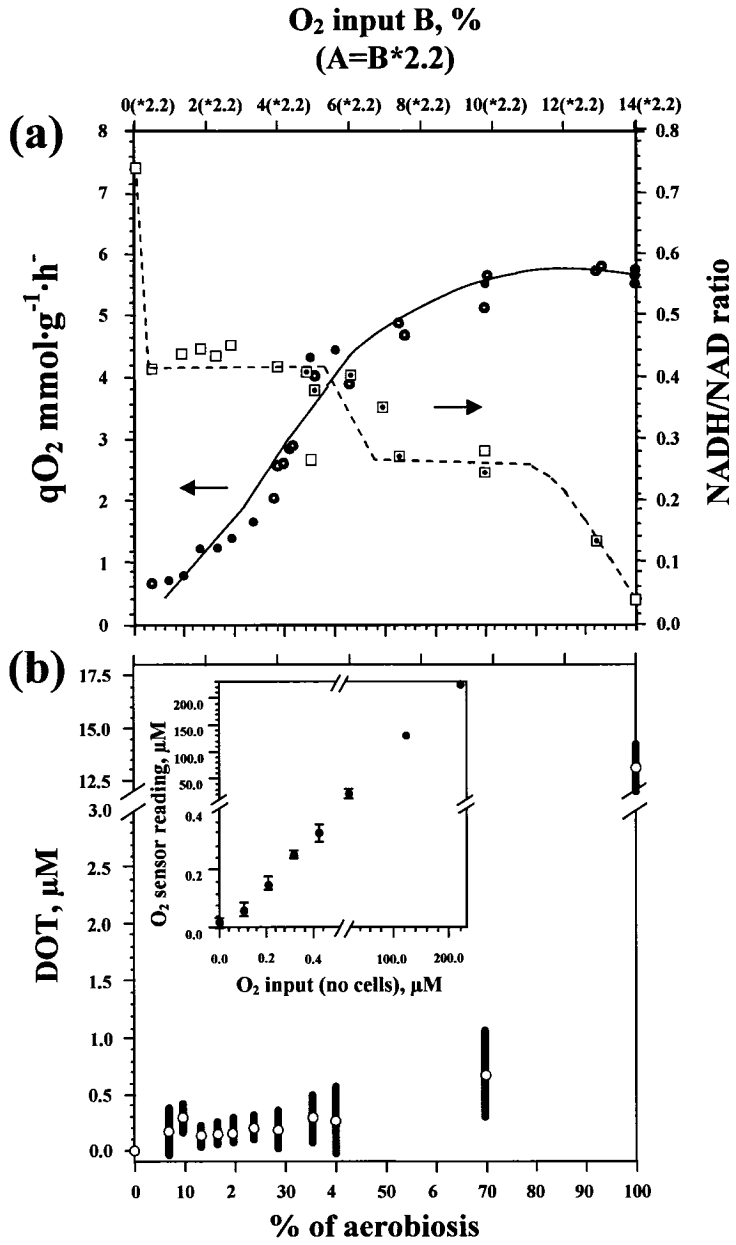

Figure 3. Specific rate of respiration, NADH/NAD ratio, and DOT in response to a change in the oxygen supply in E. coli chemostat cultivations. (a) Changes in the specific rate of respiration (qO_2, mmol/g DCW/h; ●, chemostat A; ○ chemostat B) and intracellular redox state (NADH/NAD ratio; □, chemostat A; □ dot, chemostat B); (b) Residual DOC with increasing O_2 supply within 0-100% aerobiosis. Culture volume of chemostat A, 1250 mL; chemostat B, 1380 mL. Upper x axis, actual percentage of O_2 in the inflowing gas in chemostat B. Bars, amplitude of fluctuations in DOT. (Inset) Control of O_2 electrode sensitivity in the low and high ranges. The control was performed in the absence of cells. Adapted from Alexeeva, *et al.*

2.2 Microaerobicity

The degree of microaerobicity is an important parameter to be quantified to distinguish between oxygen limited and oxygen starved conditions since DOC reads 0% in both cases. Yet, because it is difficult to define, it seems that the measurement of microaerobicity is not standardized among different research groups. For some experiments, the measure of microaerobicity is not as critical for the purpose of their study. For studies that test the effect of low oxygenation concentrations for microbial fermentation process, whether testing for cell growth, protein expression, or heterologous production, tools for measuring and regulating accurate and concise level of oxygen availability are necessary.

2.2.1 Dissolved Oxygen Concentration

Wang [29] used a DOC of 1 to 3% of air saturation in their laboratory-scale experiments to refer to oxygen-limited condition for the production of poly(3-hydroxybutyrate) (PHB) in *E. coli*. The fed-batch process was scaled up to a 50-L bioreactor where the cultivation was carried out at 20% initially but dropped to 0% DOC due to oxygen transfer limitations. At this point both the stir rate and oxygen enrichment had reached maximum output. The results showed that there was no significant difference in the volumetric productivity at the 2-L and the 50-L scales with 3.2 and 2.8 g PHB/L/h, respectively. The study concluded that no detrimental effect of oxygen limitation was observed. The run was carried out at 0% DO for 21 hours but no measure was taken to determine the degree of oxygen restriction, nor the difference in oxygen

availability between the two scales. This study showed that DO measurement alone cannot discriminate between oxygen limitation and oxygen starvation.

2.2.2 Airflow Input

Cheng [27] tested polymer material1,3-propanediol (1,3 PD) production by *Klebsiella pneumoniae*, a facultative anaerobe like *E. coli*, under different aeration rates. A strict anaerobic process was used as a control where 100% N_2 was sparged at 0.2 vvm (volume gas/volume liquid/min). Microaerobicity was varied by gradually increasing airflow from 0.1 vvm up to 0.6 vvm all at constant 150 rpm stir rate. The effect of oxygen delivery rate on 1,3 PD production from glycerol was measured. This is the most straight forward method to vary microaerobic conditions where degree of oxygen supply to the cells is assigned at the inlet. From the results shown in Table 1, Cheng concluded the condition with N_2 supplied into the bioreactor gave the highest 1,3 PD yield and productivity [27]. The results measured the effect of oxygen supply on product formation, but the relationship of airflow and oxygen availability in liquid medium for cells was not determined.

Table 1. 1,3 PD yields and productivities in batch cultures by *Klebsiella pneumoniae* under N_2 flow or airflow. Adapted from Maury, *et al.*

		PD yield (mol mol^{-1} glycerol)	PD productivity (g l^{-1} h^{-1})
With N_2	(0.2 vvm)	0.54	0.62
With air	(0.1 vvm)	0.52	0.53
With air	(0.2 vvm)	0.52	0.62
With air	(0.4 vvm)	0.46	0.55
With air	(0.6 vvm)	0.41	0.57

2.2.3 $pO_{0.5}$ Values

In the study conducted by Becker [23,30], the formation of the fermentation products in *E. coli* was studied as a function of the O_2 tension in a batch oxystat. The pO_2 (DO) range of 0.2 to 212 millibars (i.e., air saturation, 100% DO) was screened. The pO_2 was held constant by alternating supply of air and nitrogen between two valves. Products including acetate, formate, ethanol, lactate, and succinate were measured under oxic growth (aerobic condition) and anoxic growth (strict anaerobic condition). The pO_2 values that gave rise to one-half maximum amount of the products were determined and assigned as "$pO_{0.5}$" [30], somewhat analogous to Michaelis constant (K_m) derived from one-half V_{max} of enzyme kinetics. The work was initiated to obtain a quantitative measure for the effect of O_2 on transcriptional regulator in *E. coli* for anaerobic metabolism. The $pO_{0.5}$ value signifies the switch from aerobic to anaerobic respiration, the transition point of oxygen regulation [23]. With this method, the degree of microaerobicity was characterized based on the products generated rather than the oxygen concentration or delivery rate. This may be useful for setting up flask models

with different degrees of aerobicity or assessing the degree of aerobicity in facilities with poor process controls (non-uniform mixing, variable aeration). The $pO_{0.5}$ values were 0.2-0.4 mbar for lactate, succinate, acetate, and ethanol, 1 mbar for formate [30]. The products concentrations at various DOT are plotted in Figure 4 and their corresponding $pO_{0.5}$ values are listed on Table 2.

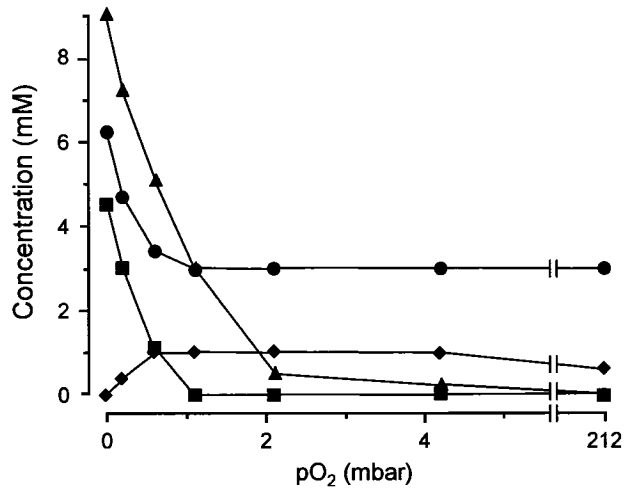

Figure 4. Fermentation products in the supernatants of *E. coli* as a function of pO_2 during growth in oxystat cultivations. Products determined at $OD_{578} = 0.5$ (▲ formate, ● acetate, ■ ethanol, ♦ fumarate). Adapted from Becker, *et al.*

Table 2. Fermentation products of *E. coli* after growth under oxic and anoxic conditions, and $pO_{0.5}$ values for half-maximal product formation. Adapted from Becker, *et al.*

Product or enzyme	Products (mM)		$pO_{0.5}$ (mbar)
	Oxic growth	Anoxic growth	
Acetate	3.0	6.2	0.3
Formate	0	9.0	1.0
Ethanol	0	4.5	0.4
Lactate	0	0.7	0.2
Succinate	0	0.6[a]	0.2
Pyruvate	0	0	-
Pyruvate formate-lyase (*pfl*)	-	-	5.0
Alcohol dehydrogenase (*adhE*)	-	-	0.8

[a]Maximal concentration, measured at 4.2 mbar O_2 in the medium

2.2.4 Aerobiosis

DOT and actual oxygen input are not good parameters to indicate actual oxygen availability in the culture. Data obtained from the use of oxygen input as a measure do not take oxygen transfer rate into account. Likewise, when the data depends on DO measurement, it is difficult to test cell responses in the low oxygen supply range. To set the accurate measure of microaerobicity during chemostat experiments, Alexeeva [21] applied the concept of aerobiosis. The key observations that led them to the definition of aerobiosis were the following: 1) different experimental setups such as alteration of the geometry of the bioreactor required different oxygen supply to achieve the same physiological response of the cells, and 2) the condition where increasing oxygen supply no longer effected the cells could be determined [21]. The microaerobic range was defined between 0 and 100% aerobiosis where 0% was equivalent to 100% N_2

(anaerobic). On the other end, 100% aerobiosis was referred to as the minimum oxygen input required to reach complete aerobic behavior, with only CO_2 as the end product. The percent aerobiosis in between 0-100% represented the fraction of oxygen in the flowing gas relative to oxygen input at 100% aerobiosis. As shown in Figure 3 (a), this technique allowed two separate chemostat runs with different volumes to demonstrate the same results for specific rate of respiration and NADH/NAD ratio, independent of oxygen concentration in the inflowing gas. The exact correlation of DOT (μM) to percent aerobiosis is illustrated on Figure 3 (b). The DOT was monitored using a polarographic O_2 sensor with a detection limit of 100 nM and accuracy within 30 mM. Measurement of percent aerobiosis goes a layer deeper in figuring the degree of microaerobicity. The drawback to its application may be that the condition for 100% aerobiosis changes with different organisms and individual strains, therefore the aerobiosis range needs to be established *apriori* for each strain by trial and error.

2.2.5 Oxidation-Reduction Potential

As an alternative to DO measurements in bioprocesses, the measurement of oxidation-reduction potentials (E) has been proposed as a useful index to express the degree of oxygen availability under a limited oxygen supply [31,32]. A standard DO sensor electrode does not precisely monitor oxygen tension below 0.01 atm (4.7% DO) [31,32] which led Shibai to look for a different process parameter to determine oxygen availability in liquid medium. Shibai [32] observed a close relationship between DO and E while cultivating *Bacillus subtilis*, when pH and temperature were constant. Shibai also observed changes in E which could not be explained by the change in DOC, data

tabulated in Table 3. While the change in DOC was minimal with the readings close to zero, the change in E was quantitatively determined even under limited oxygen availability. While the DO probe measures the oxidation potential of the available terminal electron acceptor (i.e., O_2), the redox probe measures the oxidation potential for all the species formed in the broth whose redox state depends on the availability of oxygen [31]. With sufficient supply of oxygen in the culture, more oxidized species will be present giving high redox potential reading. If the culture receives limited supply of oxygen, reduced species will be in abundance translating into low or negative redox values. The advantages of using a redox signal include the measurement of the overall feedback effect of the available oxygen instead of dissolved oxygen alone. A negative redox signal output gives further information regarding the broth oxidation state, providing information about oxygen availability, beyond the zero DO signal [31]. The latter attribute allowed Shibai to determine optimal E value for each fermentation product including lactic acid, 2,3-butyleneglycol, and acetoin. The use of redox potential was found to be a more useful measurement than dissolved oxygen in microaerobic processes.

Table 3. Relationship between redox potential (E) and dissolved oxygen (DOC) in 300 mL fermentation of *B. subtilis*. Adapted from Shibai, *et al.*

Condition of oxygen supply		DOC (atm)	E (mV)
Stir rate (rpm)	Rate of air flow (ml/min)		
1500	300	0.163	-50
1000	150	0.067	-68
950	150	0.031	-80
900	150	0.007	-105
870	150	Nearly zero	-157
850	150	Nearly zero	-160
800	150	Nearly zero	-175
700	150	Nearly zero	-200
600	150	Nearly zero	-230

Another research group, Dahod [31], has tested the use of redox potential side by side with the DOC measurement at the 4000-L scale. The complex medium used for the experiment contained soluble as well as insoluble organic and inorganic raw materials [31]. The signals for both E (mV) and DOC (%) were recorded throughout a penicillin fermentation cycle as change in DO within the positive range was triggered by changing airflow and pressure. Any response in DO triggered by these changes was also observed in the redox potential signal as shown in Figure 5. The application of the redox potential parameter was more favorable than the DOC under those conditions because commercial DO probes are often susceptible to failure or erratic signal behavior due to its construction [31]. A DO probe consists of a teflon membrane through which oxygen has to pass through via convection or diffusion before the signal is read by an internal cell. Failure or erratic signal behavior in DO measurement, which cannot be explained by process dynamics, could arise from internal electrode shorting, membrane fouling or

rapture, or partial blocking of the membrane surface during the fermentation run [31]. On the other hand, a redox probe is constructed like a pH probe where the electrode is in direct contact with the fluid which makes it less faulty from erratic signal behaviors.

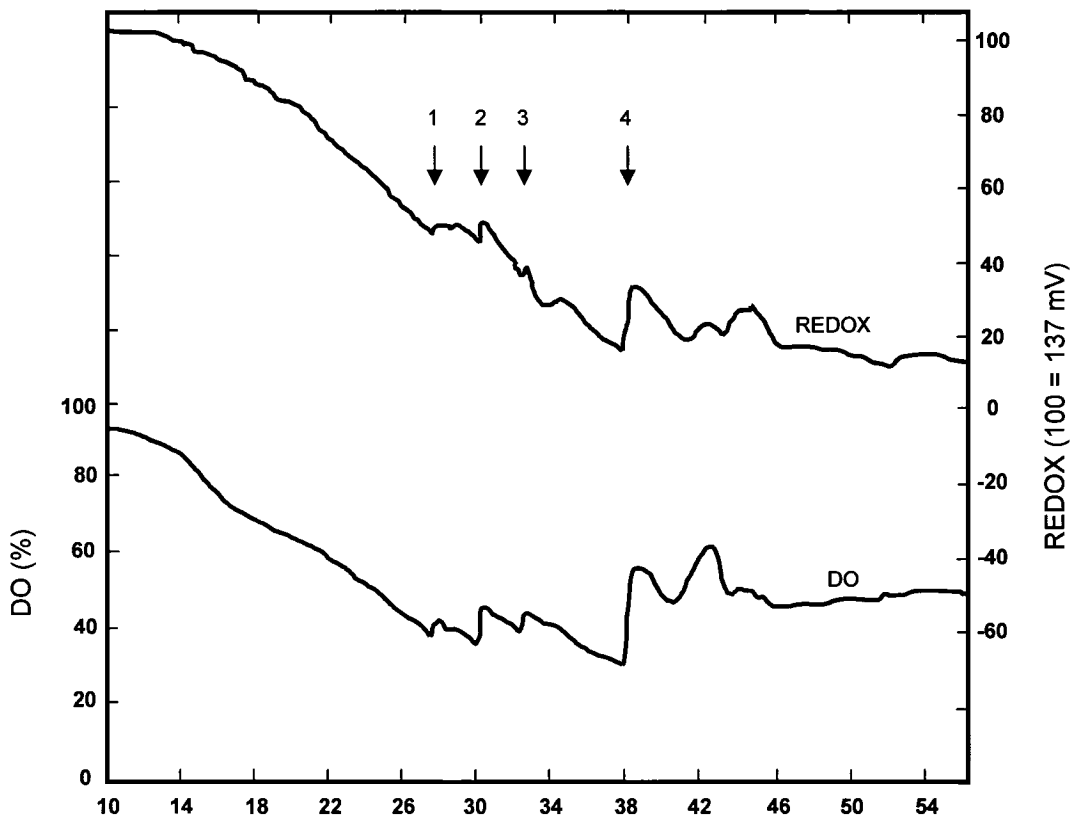

Figure 5. Dissolved oxygen and redox potential profiles during penicillin fermentation. At points 1 and 3, the fermentor airflow rate was increased; at points 2 and 4, the fermentor working pressure was increased to increase DO. Adapted from Dahod.

Though redox potential assessment in bioreactors was first published in the 1970's, it is seldom used for control purposes, thus most standard bioreactors today do not come equipped with redox measurement capability. In order to apply redox potential

as one of the process parameters, upgrades in hardware and software may be required for the bioreactor controller unit.

2.3 Fermentor System for Regulating Oxygen at Low Concentrations

As the microbes grow, demand for oxygen increases and the DOC in the medium decreases. In order to maintain the DOC (or similarly redox potential) at a set value, several strategies have been implemented in fermentor cultures. The easiest and the most commonly used feedback control process parameters to regulate are vessel pressure, agitation rate, airflow, and inlet gas composition. These parameters can be manipulated individually or in combination. However, changing parameters such as the stir rate and flow rate introduce some change in the fluid flow and shear characteristics within the fermentor, thus causing variation in gas-liquid transfer rates [33]. When operating under condition of low oxygen tension, where the probe sensitivity is at the limit, problem with DO measurements may be more pronounced by these changes. Due to these reasons, Burke [33] chose to study a system with constant stir and gas flow for cultivating yeast at low oxygen concentrations. A computer-controlled system consisting of PID (proportional-integral-differential) algorithm along with a three-way valve to mix two gases was used, as shown in Figure 6, to regulate DOC or to match cellular demand [33]. By using this regulated system, improvement in the cell growth at low oxygen concentration was demonstrated. Comparing regulated and unregulated systems at 1 μM of oxygen, the cell mass yield was two orders of magnitude higher for a regulated system, specifically 1.4 as oppose to 0.08 g (wet weight)/L [33]. A similar tool could be useful

for cultivation of *E. coli* under microaerobic conditions to support the increase in oxygen demand proportional to the increase in cell mass.

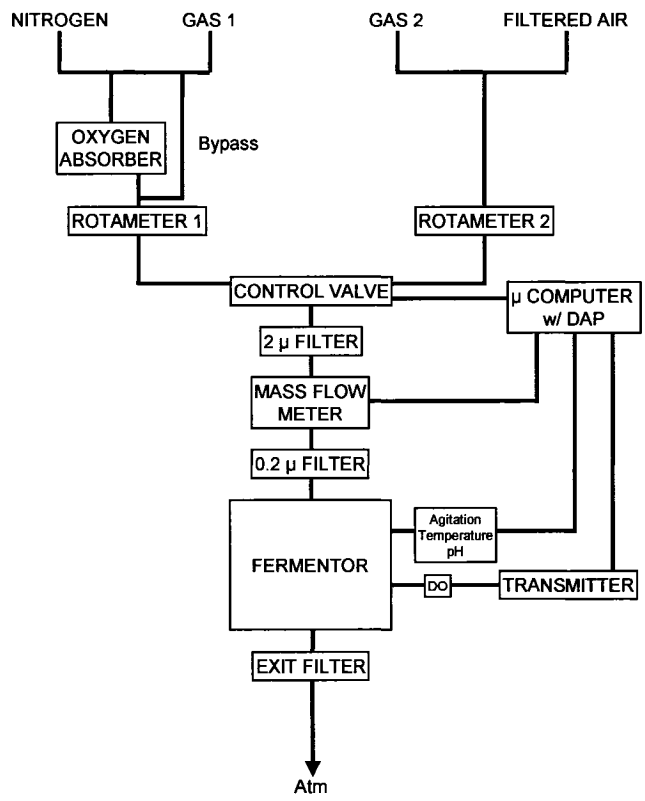

Figure 6. Flow diagram of gas flow train with three-way valve and control system used to regulate low DOC; DAP, data acquisition processor. Adapted from Burke, *et al.*

2.4 Summary of Literature Review

Aerobic processes which support high cell density are best suited for the production of high value fermentation products, where yield on carbon is not a consideration and the production cost is dwarfed by the product value. Strictly anaerobic processes are most effective when the product of interest is produced by the cell to generate ATP or to act as an electron acceptor to regenerate NAD. Under these

circumstances, product yield on carbon frequently approaches theoretical maximum and commodities such as lactate and ethanol can be generated cheaply by fermentation [6]. Heterologous production of isoprenoids will require oxygen for generation of ATP and as an electron acceptor. However, it may be possible to achieve the high yields of product from carbon that is characteristic of anaerobic processes by restricting oxygen availability to the isoprenoid fermentation.

Table 4 summarizes the process parameters that can be used to measure or vary microaerobicity. Different parameters are used for different applications. Tabulated advantages and disadvantages illustrate when the parameter is useful and when it has constraints.

Table 4. Summary of process parameters used to vary or measure microaerobicity.

Parameters that measure/vary microaerobicity	What it is/measures	Advantages	Disadvantages	References
Dissolved oxygen tension (DOT)	DO sensor measures percent dissolved oxygen in liquid medium	Useful for aerobic processes with positive DO percent (>5%)	Not possible to discriminate within a low O_2 supply range; susceptible to failure at industrial scale	[31,32]
Airflow input	Change in rate of airflow varies microaerobicity	Consistent measure of O_2 inflow run to run; non-strain dependent	Input based: ignores O_2 transfer rate, O_2 availability in liquid medium	[21,27]
$pO_{0.5}$ (chemostat)	Degree of microaerobicity characterized by product generation; $pO_{0.5}$ value signifies switch to anaerobic respiration	Useful in assessing microaerobicity in flask models, facilities with poor process control	Product based: different $pO_{0.5}$ for each product	[30]
Percent aerobiosis (chemostat)	100% aerobiosis set at normalized minimum O_2 input resulting in complete aerobic behavior	Accurate measure of O_2 availability; Independent of reactor shape or volume	Strain dependent; Aerobiosis range established by trial and error	[21]
Oxidation-reduction potentials (E)	E as an index to O_2 availability; Redox probe used to measure E (mV)	More reliable parameter than DO; Change in E quantitatively determined under low O_2 supply; Lower detection capability than DO sensor	pH and temperature must be steady for accurate reading; Redox setup not standard for bioreactor; Require upgrade in hardware	[31,32]

CHAPTER THREE
HYPOTHESIS, OBJECTIVES, AND JUSTIFICATION OF EXPERIMENTAL WORK

Some isoprenoids have potential as biofuels molecules and the production of these products may be most economical in a microaerobic process. The goal of this research is to develop a platform microaerobic fermentation process for biofuels (secondary metabolite) producing heterologous *E. coli* strains which can be scaled up eventually into an existing industrial plant.

3.1 Hypothesis

The hypothesis is that microaerobic fermentation process can capture the high yield of product from carbon that is characteristic of anaerobic fermentation processes, despite the fact that the desired fermentation products do not necessarily result in the generation of ATP or the regeneration of NAD. The mevT pathway used in this work does not generate ATP but regenerates NADP for making mevalonate (Figure 7). The hypothesis will be tested by restricting oxygen in the cultivation of an *E. coli* strain that is engineered to overproduce mevalonate. From the literature review on aerobic fermentation, more cells and fewer products are anticipated. In the case of strictly anaerobic cultivation, little or no growth and production are expected due to lack of an electron sink (NAD) and low ATP production. However, Alexeeva [21] showed that just a slight feed of oxygen into the bioreactor is sufficient to reduce the NADH/NAD ratio drastically. Therefore, under microaerobic conditions, an increase in the production of mevalonate compared to aerobic or anaerobic cultivation is expected. Microaerobic

processes will also reduce cell growth (low cell density growth) and reduce CO_2 generation.

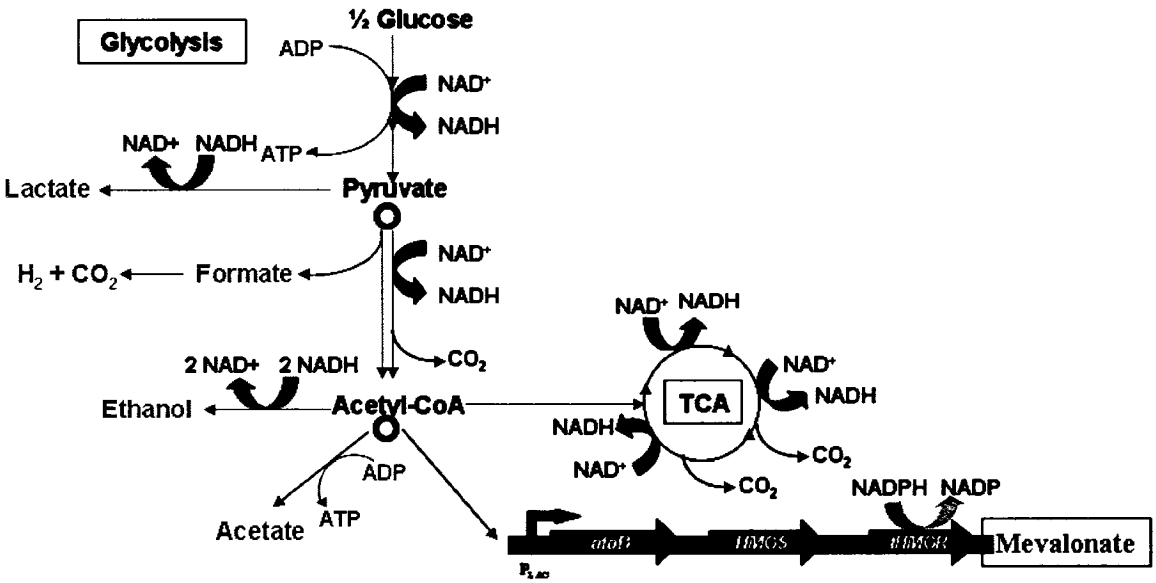

Figure 7. Metabolic pathways for engineered *E. coli* strain harboring the top mevalonate pathway.

From the above hypotheses, the production of mevalonate is believed to be dependent on oxygen concentration. Some possible scenarios are the following: 1) a direct linear relationship between oxygen concentration and mevalonate production, or 2) there is a minimum requirement of oxygen concentration before any mevalonate is produced, illustrated in Figures 8 (a) and (b), respectively. The question to be answered: What degree of oxygen restriction is tolerated by *E. coli* strains for the production of recombinant proteins and, thus, secondary metabolites (e.g., fuel molecules)?

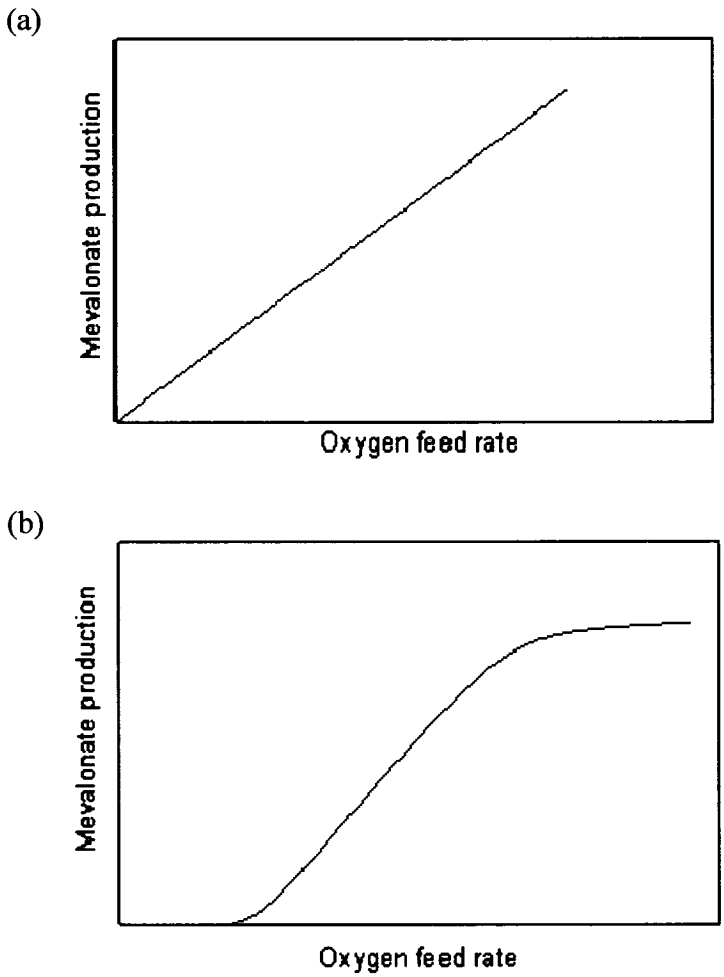

Figure 8. Hypothetical relationships between mevalonate production and oxygen feed rate. (a) A linear relationship shown between oxygen feed rate and mevalonate production, (b) Minimum threshold of oxygen feed rate shown for mevalonate production.

3.2 Objectives of the Experimental Work

A detailed study of anaerobic and microaerobic fermentations of heterologous production of mevalonate in *E. coli* will be undertaken. The main objective of the study is to define appropriate aeration strategies in microaerobic batch process to maximize mevalonate yield on glucose. This work will establish test platforms for genetically

engineered isoprenoid fuel strains and central metabolism modifications that will channel glucose away from biomass and organic acids accumulation and toward fuel molecule production. The process developed for mevalonate production can be used for production of other potential fuel molecules and modified to suit their requirements.

3.3 Economic Justification of Experimental Work

Isoprenoids and polyketides for pharmaceutical application may have fairly expensive microbial fermentation processes involving high concentration feedstock in an aerobic process, with GMP regulations in some processes. For instance, 645 g/L of glucose was fed to a microbial process to produce 1.1 g/L of 6-deoxyerythronolide B, a precursor to antibiotic erythromycin [15]. This translates to a yield of only 0.17% (wt/wt) from glucose. The low yield and the expensive process of operation are not a factor when pharmaceutical applications are at stake, since the product is far more valuable than the raw materials.

However, with the production of biofuels, this is not the case. Because the value of the end product is inexpensive and it will be burned as a fuel, higher yield from raw materials (carbon) is required as well as low process costs, so that the product is cost competitive with gasoline. Based on the literature review, an aerobic fermentation process will support high cell density [17,18] and convert raw materials into cell mass and CO_2 gas [26] with low conversion of carbon to biofuels at high utilities costs. By designing an anaerobic or microaerobic process, product yield on raw material can be greatly improved [27]. A successful anaerobic/microaerobic process for the production of isoprenoids biofuels will be similar to the existing bioethanol process and fit into

existing industrial plants, thus saving money on capital investment. A microaerobic process will generate ATP and regenerate NAD more effectively than anaerobic process which may stimulate higher productivity of the fuel molecule by shifting carbon flow toward the pathway and away from organic acid byproducts. Low input of air into the bioreactor may be feasible at industrial scale.

3.4 Technical Justification of Experimental Work

An *E. coli* strain harboring the top pathway (mevT) of the isoprenoid pathway was used for the experiments, shown in Figure 7. The strain synthesized mevalonate as the final product from units of acetyl-CoA. The overproduction of mevalonate is necessary for overproduction of any isoprenoid biofuel. Glycolytic accumulation of the reducing equivalents, i.e., NADH, promotes the formation of fermentation byproducts under anaerobic conditions. This is a problem since the goal is to make biofuel molecules instead of the byproducts. The redox imbalance in the production of mevalonate will be solved by feeding oxygen in small amounts, i.e., microaerobic fermentation.

The effect of slow oxygen feed or zero oxygen supply in the microbial cultivation for the heterologous production of secondary metabolites has not been well characterized. There was some work done on exploring the effects of dissolved oxygen on recombinant protein production in *E. coli* [34,35] under anaerobic (100% N_2) and aerobic (0%-20% DO) batch processes; however, the microaerobic range was ignored. There were also studies conducted to see the effect of microaerobicity in *E. coli* [21,30], in recombinant *E. coli* [18], and in yeast [36,37]. In these studies, the synthesis of the fermentation

products (primary metabolites) was analyzed instead of the heterologous production of secondary metabolites, and again the full spectrum of the microaerobicity was neglected for most experiments.

What is apparent from the literature review is that there is no standardized way of measuring and defining microaerobicity among different research groups. Wang [29] calls 1-3% DO a microaerobic process while Cheng [27] sets different airflow rates (vvm) to perform microaerobic experiments without any disclosure of DO concentration in his/her work. Becker [23] and Alexeeva [21] defined their own parameter, $pO_{0.5}$ in batch oxystats and percent aerobiosis in chemostats, respectively, to determine the degree of microaerobicity in their cultures. In this work, variation in oxygen concentration was assigned in the inflowing gas, a method similar to Cheng's work, to test the microaerobic range. The percent air of the inflow gas was varied; however, the gas flow rate into the reactor at 1 vvm was kept constant for all experiments. In addition, Alexeeva's work on defining the boundaries of 100% aerobiosis was considered. Furthermore, DO concentration was monitored using a high O_2 sensor and a oxidation-reduction potential probe recommended by Shibai [32]. Redox probe measurements will hopefully distinguish among different degrees of microaerobicity and also provide a measure of biological activities or reactions.

By screening the full range of microaerobicity, an optimal aeration strategy can be identified for biofuel molecule production from fermentation. The optimal aeration process will serve as a platform tool to assess engineered strains for growth, organic acids productions, biofuels molecule production, and product yield on glucose. Measuring the

effect of oxygen delivery on mevalonate biosynthesis from heterologous enzymes, as well as developing tools for well controlled microaerobic oxygen delivery, is the first step towards determining the effect of oxygen delivery on heterologous production of more complex fuel molecules.

CHAPTER FOUR
EXPERIMENTAL DETAILS

4.1 Method of Investigation

Aerobic, microaerobic, and anaerobic fermentation processes were compared for the cultivation of heterologous *E. coli* strains that produce mevalonate, a precursor to isoprenoid biofuel molecules. First, media and process variables published by Korz [38] and Carlson [25], respectively, were tested and refined to establish some of the process variables to be used for all experiments. Secondly, aerobic and anaerobic control processes were tested. Aerobic batch fermentation process controlled at 40% DO (pO_2 = 40% of saturation) served as a basis for nutrient excess cultivation with oxygen as an abundant nutrient since no oxygen limitation to the organism has been reported at 40% DO. Under strict anaerobic fermentation, 100% nitrogen gas was sparged into the bioreactor and this is considered an oxygen starved fermentation process. Microaerobic fermentation, defined as oxygen level between no oxygen supply and 100% aerobiosis, was operated by varying the percentage of oxygen in a gas mixture of air and nitrogen going into the bioreactor. Nitrogen gas, since it is inert, was used to decrease the concentration of oxygen without changing the gas flow rate. Microaerobic fermentation was treated as a nutrient restricted fermentation process with oxygen as the only limited substrate. Finally, a low positive DO range was tested to find the operating condition close to 100% aerobiosis within the feasible positive DO range.

Samples obtained from earlier cultivations were used to trouble-shoot analytical methods on the HPLC to quantify the amount of carbon products as accurately as

possible. This information was necessary to close the carbon balance. Once the reliable analytical methods were developed, analysis of organic acids, mevalonate production, and carbon balance of all runs was completed.

Fermentation runs on control processes and key microaerobic runs were repeated as necessary to confirm the results. After the complete analyses of all runs, a microaerobic fermentation process with the best result in mevalonate yield on glucose was identified. A flow chart of the overall experimental work is shown in Figure 9.

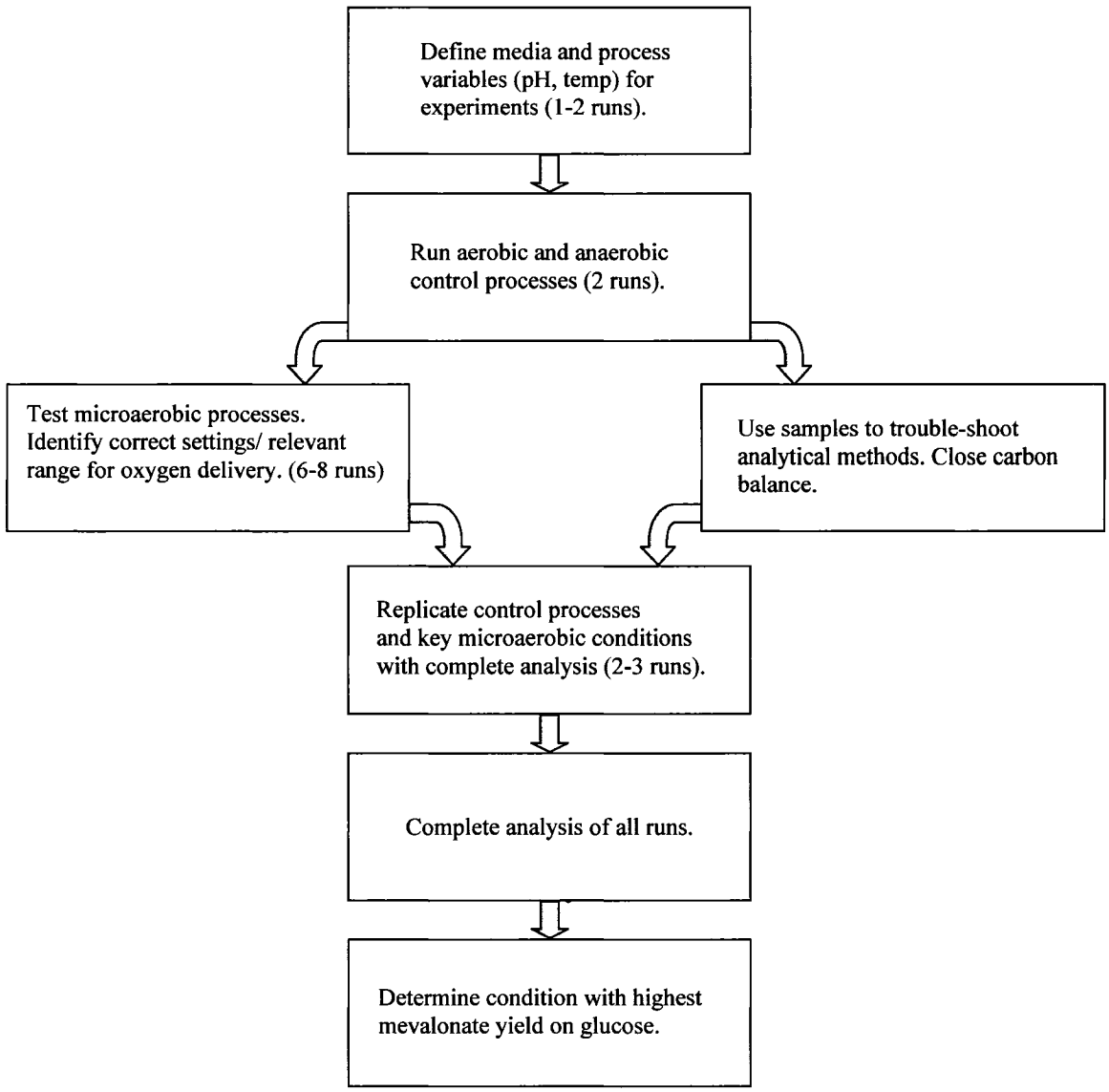

Figure 9. Proposed experimental flow.

4.2 Materials and Experimental Procedures

A schematic overview of one fermentation run is summarized in Figure 10.

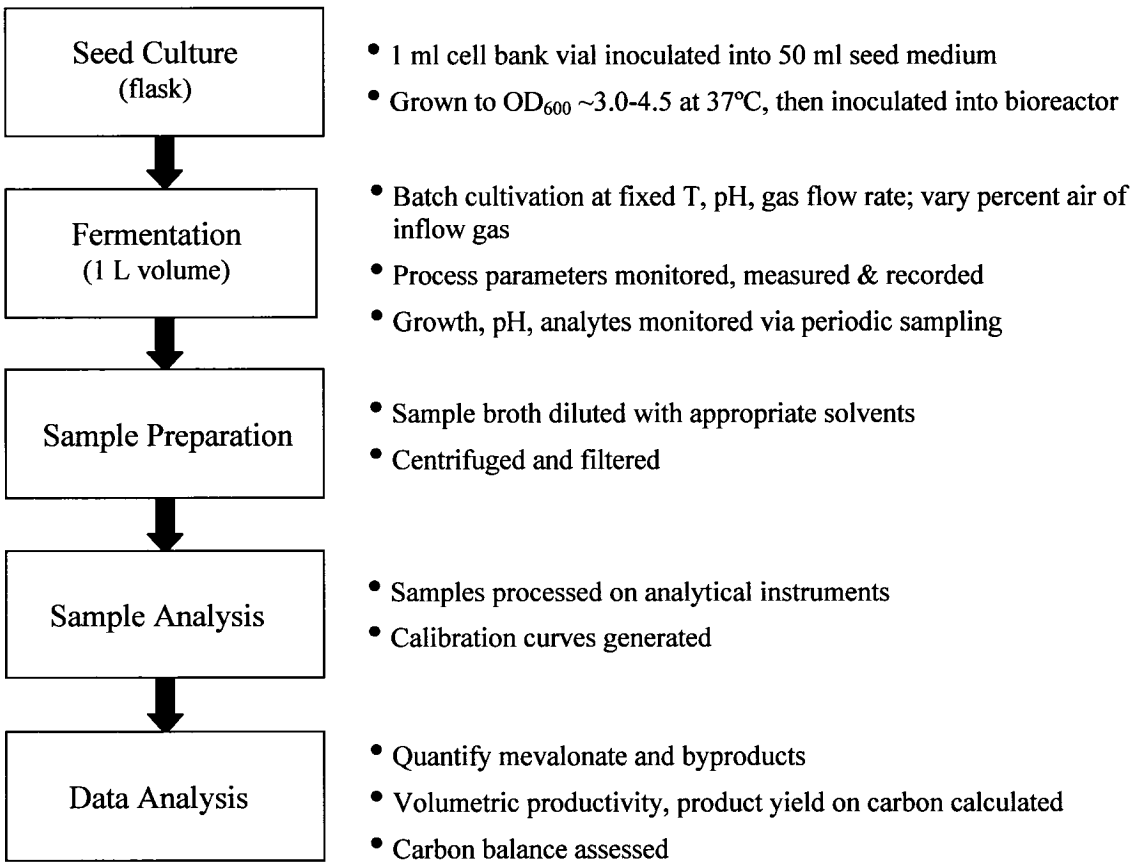

Figure 10. Flow diagram of a single fermentation run.

4.2.1 Strain and Media

E. coli strain B254 in a DH1 host harboring a plasmid containing the top mevalonate pathway (mevT) including genes of atoB, HMGS, and tHMGR was used for this work. The plasmid has a lac promoter inducible by IPTG (isopropyl β-D-1-thiogalactopyranoside) as well as resistance against T1 phage and antibiotics carbenicillin and kanamycin.

M9 medium was used to grow seed cultures. A chemically defined medium that supports high cell density fermentation (OD_{600} value of 200) [38] was used as a reference to formulate a medium that supports low cell density fermentation. To start, medium concentration diluted by four-fold was used for the experiment. Both seed and fermentation media (containing batch medium and post sterile additions) are shown in Tables 5 and 6. Trace metal (TM) stock solution composition is listed in Table 7. A 50 mL overnight seed culture of strain B254 grown in an aerated shake flask to OD_{600} value of 3.0-4.5 at 37°C and 250 rpm was used to inoculate the bioreactor (Sartorius Biostat B Plus) containing 1 L of fermentation medium. Batch medium was autoclaved in the bioreactor and post sterile additions were filter sterilized and injected into the bioreactor after the autoclave cycle. Glucose was the sole source of carbon supplied in the medium.

Table 5. M9 seed medium components.

Component	M9 medium (per L)
Glucose	8 g
Na_2HPO_4 $7H_2O$	12.8 g
KH_2PO_4	3 g
NaCl	0.5 g
NH_4Cl	1 g
$MgSO_4$	2 mmol
$CaCl_2$	0.1 mmol
Thiamine	0.1 ug
MOPS buffer pH 7.4	100 mmol
$(NH_3)_6Mo7O_{24}$ $4H_2O$	3.7 ug
H_3BO_4	25 ug
$CoCl_2$	7.1 ug
$CuSO_4$	2.4 ug
$MnCl_2$	16 ug
$ZnSO_4$	2.9 ug
$FeSO_4$	0.28 mg

Table 6. Chemically defined fermentation media: (a) batch medium and (b) post sterile additions.

(a)

Component	Concentration (g/L)
KH_2PO_4	4.2
K_2HPO4 $3H_2O$	15.7
Citric acid	1.7
$(NH_4)_2SO_4$	2
0.5 M EDTA (µl/L)	57.5

(b)

Component	Concentration (g/L)
batch TM (mL/L)	5
glucose	30
$MgSO_4$ $7H_2O$	0.3
thiamine	0.0045

Table 7. Batch trace metal solution composition.

Component	Concentration (g/L)
$CoCl_2\ 6H_2O$	0.25
$MnCl_2\ 4H_2O$	1.5
$CuCl_2\ 2H_2O$	0.15
H_3BO_4	0.3
$Na_2MoO_4\ 2H_2O$	0.25
$Zn(CH_3COO)_2\ 2H_2O$	1.3
Fe(III)citrate hydrate	10

4.2.2 Fermentation Process Variables: Fixed and Manipulated Variables

The amount of carbon (i.e., glucose) supplied in the medium was 30 g/L for all experiments. Cultivation temperature of 30°C and pH of 7.0 as suggested by Carlson [25] was tested initially and assigned as a set point for all experiments using the Sartorius Biostat B Plus controller. The pH was maintained using 9.9 N ammonium hydroxide solution and 5 N sulfuric acid solution. Ammonium hydroxide was used also to served as additional nitrogen source for the cells to build cell mass. The gas flow rate remained constant at 1 vvm for all cases. The only variable that was changed for each run was the oxygen delivery varied either by using the gas-flow ratio control, or the stir rate for the DO feedback control. The process parameters including pH, temperature, stir rate, airflow, and gas-flow ratio were recorded by MFCS (mass flow control system) software throughout the course of the cultivation. The bioreactor and the controller unit are shown in Figure 11.

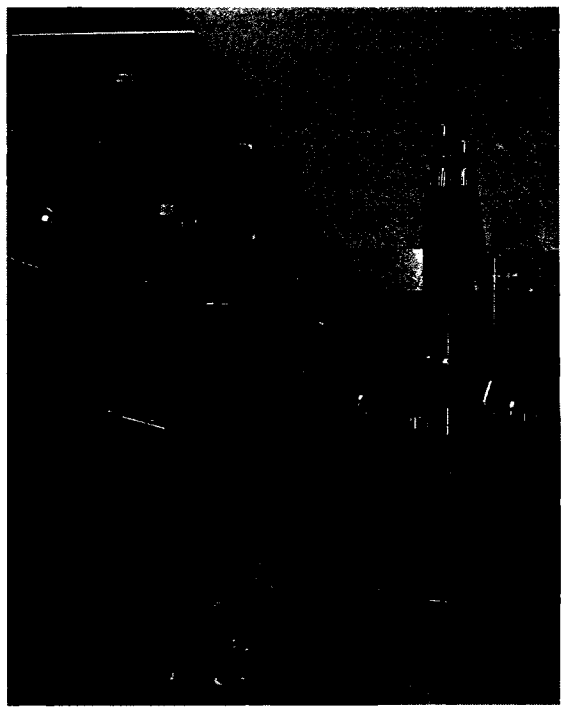

Figure 11. A 2-L vessel bioreactor with a controller unit (Sartorius Biostat B Plus).

4.2.3 Aerobic, Anaerobic, and Microaerobic Processes

For aerobic processes, a 40% DO set point was selected as the aerobic control process and a 5% DO set point was also tested additionally as a low positive DO concentration. Inflowing gas of 100% air naturally consisting of 21% oxygen was sparged into the aqueous medium at 1 vvm. The DO feedback control was applied to maintain the DO concentration at the set point by increasing the stir rate. The initial stir rate was set at 300 rpm. The DO concentration was measured using an O_2 sensor probe (Hamilton, OXYFERM FDA 225) with sensitivity between 10 ppb to saturation. The culture was induced with 1mM IPTG at OD_{600} value of ~3.0 to initiate gene expression.

For the strict anaerobic process, 100% nitrogen gas was sparged at 1 vvm into the aqueous medium prior to inoculation. A low constant stir rate of 300 rpm was maintained throughout the cultivation. Because the presence of low CO_2 concentration is known to promote cell growth in low cell density cultures [39], an additional strict anaerobic condition was tested supplementing 2% of the N_2 inflow gas with CO_2. The processes were induced with 1 mM IPTG regardless of attaining cell density of OD_{600} value of 3.0.

The spectrum of microaerobicity was tested by changing oxygen delivery concentration using the gas-flow ratio control of nitrogen and air. The O_2 availability was monitored using a high sensitivity O_2 probe with sensitivity down to 6 ppb, 6 μg/L (Mettler Toledo, InPro 6800), and the activity of the culture was measured using a redox probe (Mettler Toledo, InPro 3250SG/225/Pt1000). The cultures were induced with 1mM IPTG at OD_{600} value of ~3.0.

Aerobic, microaerobic, and anaerobic processes are illustrated with oxygen supply and DO scale in Figure 12 and corresponding fermentation process conditions are tabulated in Table 8.

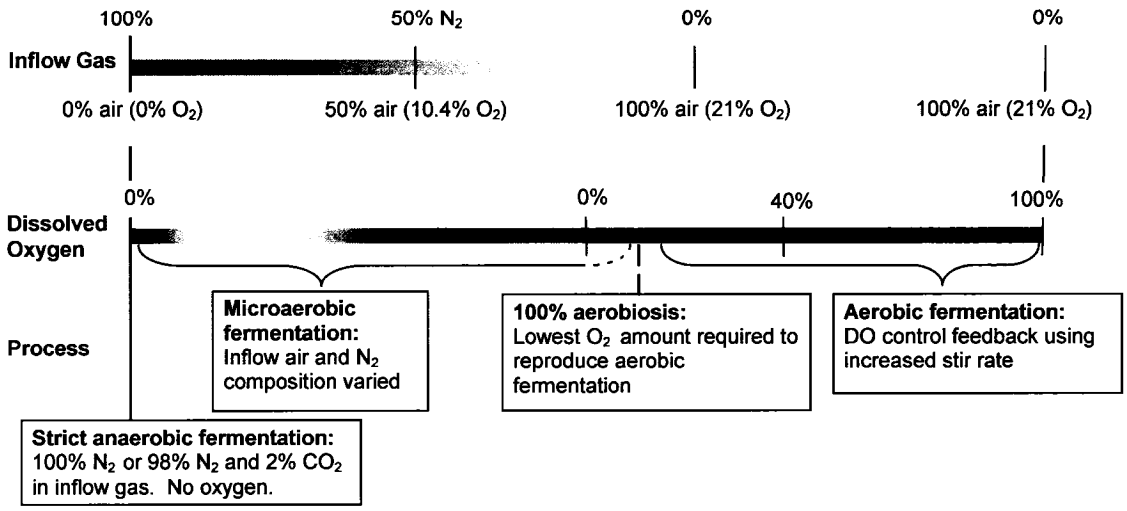

Figure 12. Variance of dissolved oxygen and inflow gas compositions for strict anaerobic, microaerobic, and aerobic fermentation processes.

Table 8. Detailed fermentation process conditions for aerobic, microaerobic, and strict anaerobic cultivation used in the experiment.

Process	Conditions	Controlled Parameters	Gas Flow Composition	# of runs
Aerobic	40% DO	DO feedback control with stir rate, start @300 rpm.	100% air (21% O_2)	2
	5% DO			2
Microaerobic	0% DO range with air supply	No DO feedback control. Constant stir rate, 300 rpm. O_2 availability measured by DO and redox probe.	100% air, 0% N_2	1
			90% air, 10% N_2	1
			70% air, 30% N_2	1
			50% air, 50% N_2	1
			35% air, 65% N_2	1
			20% air, 80% N_2	1
			10% air, 90% N_2	1
			5% air, 95% N_2	1
Strict Anaerobic	No air supplied	Constant stir rate, 300rpm.	2% CO_2, 98% N_2	1
			100% N_2	2

4.2.4 Sample Preparation and Analysis

Cell density and glucose consumption were monitored offline by taking culture samples frequently throughout each run. Cell density was measured using a spectrophotometer set at 600 nm wavelength using an appropriate dilution of a fresh culture. Instant glucose measurement was taken using Nova Bioprofile 300A by injecting the diluted supernatant. The broth samples were aliquoted in 1 mL volumes for each time point and stored at -20°C for other analyses.

HPLC was used to quantify levels of organic acids, sugars, and mevalonate with either a UV detector set at 210 nm or a RI (refractory index) detector. An ion exclusion column (50 angstrom, 7μm, 7.8 x 300 mm) packed with PSDVB by IC-Pak ™ was used

to separate organic acids, aliphatic alcohols, and glycols with a dilute sulfuric acid mobile phase (15 mM). The ion exclusion chromatography allowed the separation of weakly ionized acids based on differences in pK_a values [40]. The column also allowed for separation by size and hydrophobicity; separation was enhanced with functional groups in the resin structure which promoted hydrogen bonding and adsorption [40]. A flow rate of 0.6 mL/min at 65°C was applied over 25 min to elute all products.

For HPLC sample preparation, a frozen 1 mL fermentor broth sample was thawed and diluted five-fold using 18.75 mM sulfuric acid solution for a final concentration of 15 mM sulfuric acid to match the concentration of the mobile phase solution. Cells were removed by centrifugation and filtration prior to loading on HPLC.

A YSI analyzer was used to measure the concentration of ethanol in the fermentor samples. The YSI used enzymatic methods for analysis, and sample processing requires removing cells and potentially diluting samples to keep them within the instruments range. The Nova bioprofile 300A was used to measure glucose (enzymatically), acetate (electrochemically), ammonia (electrochemically), and phosphate (photometrically) concentrations [41]. This instrument also required cells to be removed and supernatant to be diluted so that the analyte of interest was the right analytical range. YSI and Nova bioprofile measurements were used as a back up to confirm HPLC data.

The molar flow rates of inlet and outlet gas compositions were measured via off-gas mass spectrometer (depending upon detection limit). Based on these flow rates and concentration of inert gas, oxygen, and CO_2 at the inlet and outlet, oxygen uptake rate (OUR), carbon dioxide evolution rate (CER), and respiratory quotient values (ratio of

CER to OUR) were calculated and recorded on-line through the MFCS software throughout the cultivation. The OUR is the difference between the rates at which oxygen enters and exits the fermentor per liquid volume. The CER is calculated in a similar manner except the inlet CO_2 is subtracted from the outlet CO_2. The formula used to calculate OUR is derived from Equations 2 (a) and (b), and shown in Equation 2 (c) [42]. The formula for CER is shown in Equation 3.

$$OUR = (F_i*[O_2]_i - F_o*[O_2]_o) / V * K \qquad \text{Equation 2 (a)}$$

$$F_o = F_i*[I]_i / [I]_o \qquad \text{Equation 2 (b)}$$

$$OUR = ([O_2]_i - [I]_i*[O_2]_o/[I]_o) * F_i / V * K \qquad \text{Equation 2 (c)}$$

$$CER = ([I]_i*[CO_2]_o/[I]_o - [CO_2]_i) * F_i / V * K \qquad \text{Equation 3}$$

F is the gas flow rate, V is the fermentor volume, K is the conversion constant, $[O_2]$ is the concentration of the oxygen, $[CO_2]$ is the concentration of carbon dioxide, [I] is the concentration of inert gas, subscript i and o stands for inlet and outlet, respectively.

The summary of instruments and analytes is shown in Table 9. The carbon containing products used to determine the carbon balance are shaded.

Table 9. List of analytes and parameters detected by instruments.

	HPLC	Nova Bioanalyzer	YSI	Off-gas Analyzer
NH_4+		x		
PO_4		x		
glucose	x	x		
ethanol	x		x	
acetate	x	x		
lactate	x	x		
formate	x			
succinate	x			
mevalonate	x			
CO_2				x
OUR				x
CER				x

4.2.5 Data Analysis

The following results were evaluated from the data collected from analytical instruments. First, the difference in oxygen delivery using the gas flow ratio control and the DO feedback control was assessed. Secondly, in the biological system, the effect of oxygen delivery or DO saturation on 1) glucose consumption and cell growth, 2) organic acids formation, 3) heterologous mevalonate production, specific productivity, and mevalonate yield on glucose ($Y_{P/S}$), biomass ($Y_{P/X}$), and growth yield on glucose ($Y_{X/S}$), and 4) OUR, CER, and RQ were evaluated.

In addition to evaluating the biological data, percent carbon recovery was calculated to ensure material balance around carbon and to trace all the carbon in the products. The carbon balance was calculated by summing up all the carbon containing metabolites detected on the analytical instruments listed on Table 10, in units of moles of

carbon per L, and comparing it to the starting carbon concentration as shown in Equation 4. The chemical composition of the *E. coli* cells was estimated as $C_4H_7O_2N$ per mole or 39.8 mmol C per gram DCW [43]. A correlation between OD_{600} and dry cell weight (DCW) was established by sampling 1.5 mL of high cell density *E. coli* culture at different time points. The cell broth was sampled into completely dried, tared eppendorf tubes and centrifuged into a cell pellet. The cells were washed once with water and centrifuged again. The cell pellet was dried in an 80°C incubator for 3 days before weighing. The dried pellets and tubes were weighed and the tube weight was subtracted. Dry weight (mg) was then divided by volume (1.5 mL) to give cell mass as DCW (g/L).

$$Carbon\ recovery\ (\%) = \frac{\Sigma\left[products\ (M) * \frac{moles\ C}{mole}\right]}{initial\ glucose\ (M) * \frac{6\ moles\ C}{mole}} \times 100 \qquad \text{Equation 4}$$

Table 10. List of products, their molecular weight, and their number of carbons per mole used in the carbon balance.

Products	MW	# of Carbon
biomass ($C_4H_7O_2N$)	101	4
lactate	90	3
formate	46	1
acetate	60	2
ethanol	46	2
succinate	118	4
CO_2	44	1
glucose	180	6
mevalonate	148	6

In addition, tools for measuring microarobicity were assessed. Comparison and contrast was made between the DO and the redox measurements. The signal response to the oxygen availability during cultivation and differences in redox potential drop according to the amount of oxygen supplied was studied.

The only criteria for selecting the best microaerobic condition for the strain tested was based on the mevalonate yield on glucose ($Y_{P/S}$).

CHAPTER FIVE
RESULTS AND DISCUSSION

5.1 Variation of Oxygen Delivery using Gas-flow Ratio Control and Dissolved Oxygen Feedback Control

Different amount of oxygen were delivered to the bioreactor by using the dissolved oxygen feedback control loop for the aerobic process, or by varying the composition of inlet gas mixture to the bioreactor (nitrogen gas to air percentage) for strict anaerobic and microaerobic processes. The 100% N_2 was used for the strict anaerobic process while percentages between 95% and 0% N_2 were applied for microaerobic processes. The actual oxygen delivery into the reactor was calculated by MFCS using 20.8% oxygen composition in air and recorded throughout the cultivation as shown in Figure 13. In the legend, aerobic conditions are defined by percent DO and represented in dark blue colors; microaerobic conditions are defined by percent nitrogen gas in the inlet gas, e.g., 0% N_2 indicates 100% air in the inlet gas, 90% N_2 indicates the remaining 10% is air, shown from light blue to green to orange to illustrate different degrees of micoaerobicity; strict anaerobic conditions contained no air, thus no oxygen, in the inflow gas and are graphed in pink and red. With decreasing amount of nitrogen gas supplemented for microaerobic conditions, increasing amount of oxygen flow rate was observed. The conditions of 40% DO, 5% DO, and 0% N_2 all had 100% air supplied corresponding to approximately 9 mM/min oxygen. The difference among the three conditions is apparent on Figure 14 as the stir rate climbed to maintain the set percent DO under the aerobic 5% and 40% DO conditions. Increasing the stir rate caused air bubbles to break up into smaller particles, thus increasing the dissolved oxygen concentration in

the liquid medium. For conditions between 0% N_2 and 100% N_2, the stir rate was maintained at a constant 300 rpm throughout the entire cultivation since the dissolved oxygen parameter was not controlled; DO was allowed to drop to zero as response to cell respiration (see Section 5.10 for DO profiles).

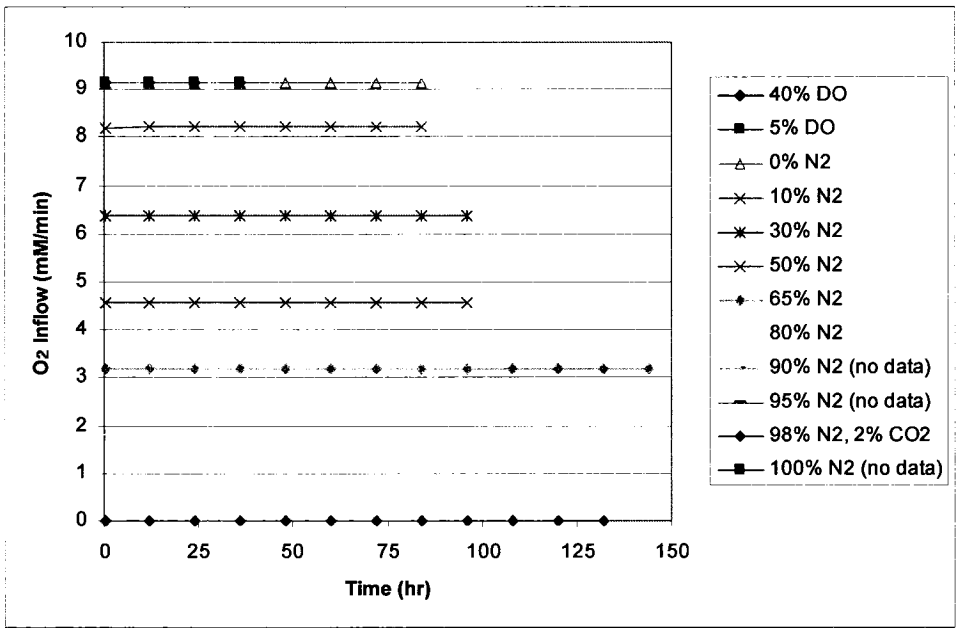

Figure 13. Oxygen flow rate (mmol/L/min) into the bioreactor as supplied by air for aerobic, microaerobic, and anaerobic processes as recorded by MFCS. Data was not collected for 90%, 95%, and 100% N_2 conditions.

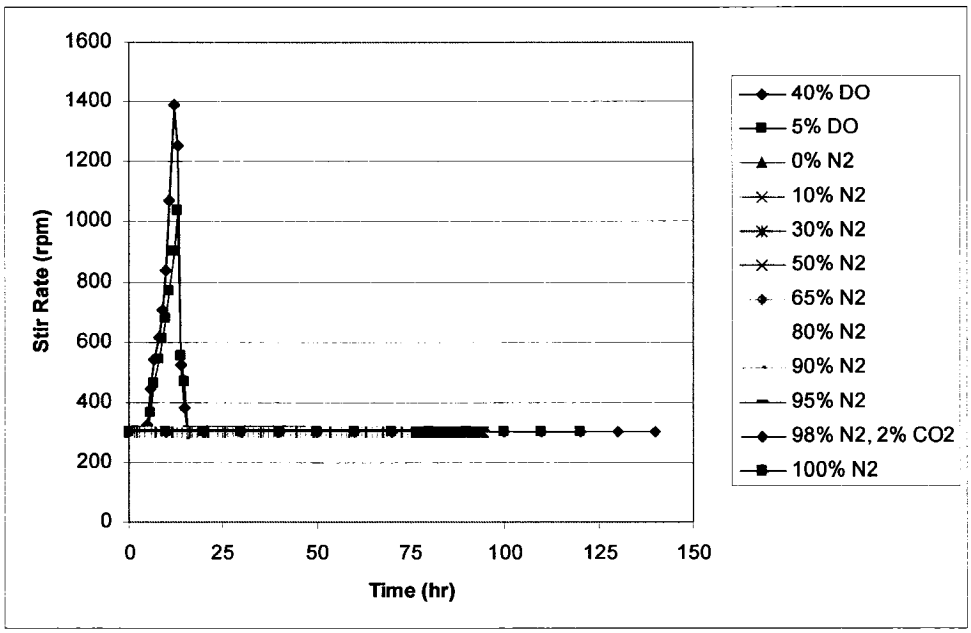

Figure 14. Impeller stir rate recorded by MFCS for aerobic, microaerobic, and anaerobic processes.

5.2 Effect of Aerobic, Microaerobic, and Strict Anaerobic Processes on Glucose Consumption and Cell Growth

Glucose is most commonly catabolized via the glycolysis pathway to make ATP for cellular energy. During the course of ATP production, NAD is regenerated in complex I of the electron transport system chain [20] to carry out many cycles of glycolytic reactions as shown in Figure 15. In aerobic cultivation, the presence of oxygen molecules effectively allows the reoxidation of NADH to regenerate NAD, promoting fast consumption of glucose. This phenomenon was observed with 40% and 5% DO conditions. With a batched glucose of 30 g/L in the medium, aerobic conditions consumed the entire supply within 24 hrs after inoculation. The microaerobic conditions (up to 65% N_2 condition) depleted glucose by 32 hrs as shown in Figure 16. For microaerobic conditions higher than 80% N_2, it took longer than 50 hrs to break down the

supplied glucose. This lag in glucose depletion suggested limitation of NAD cofactor regeneration under low limited oxygen supply.

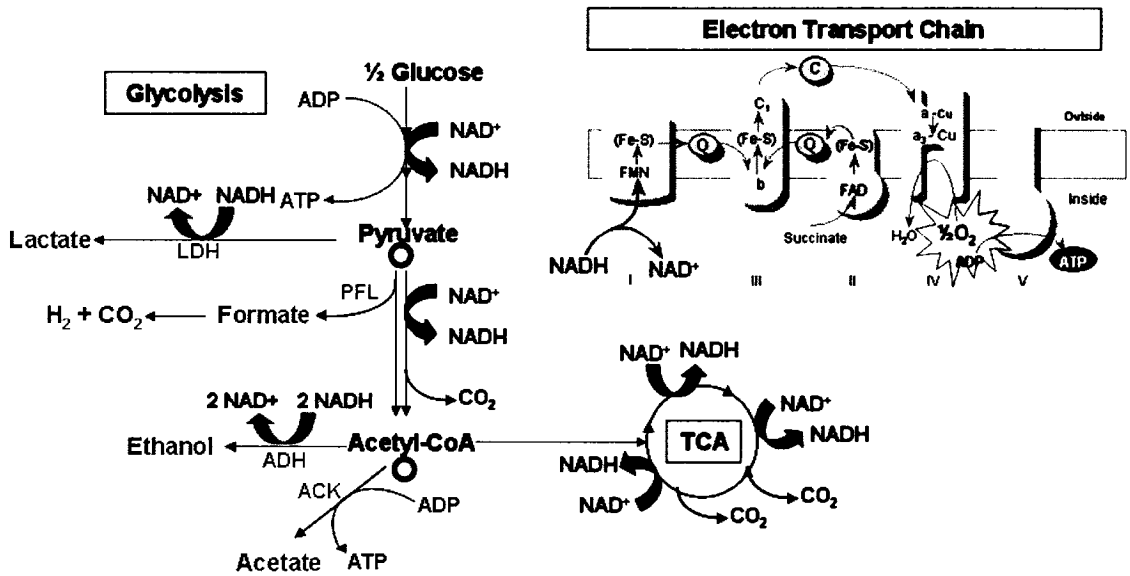

Figure 15. Glucose metabolism via glycolysis, TCA cycle, and ETS chain in *E. coli* [20]. Anaerobic (left) and aerobic (right) routes. Open circles indicate branch points of the respiratory and fermentative catabolism [21].

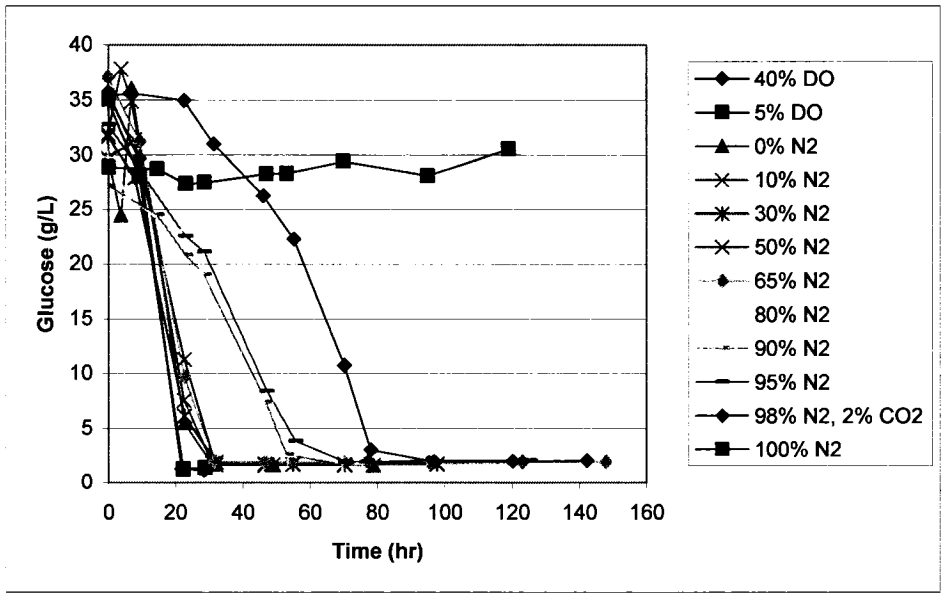

Figure 16. Glucose concentration in the medium post inoculation under aerobic, microaerobic, and anaerobic processes. Concentration determined by HPLC (see Section 5.6).

Under the strict anaearobic condition (100% N_2), no utilization of glucose was observed throughout the 120-hr cultivation. This corresponded to no cell growth over 120 hrs as shown in Figure 17. Metabolism was not active in that process. However, eventual consumption of glucose as well as cell growth was observed in the 2% CO_2, 98% N_2 anaerobic condition. The glucose was entirely consumed by 100 hrs and the culture was able to grow to OD_{600} of 3.5. A low concentration of dissolved CO_2 gas in the medium was necessary to promote cell metabolism and growth in the strict anaerobic condition. This phenomena was explained by Chen [39] as heterotrophic CO_2 fixation required to replenish the TCA cycle intermediates. Necessary CO_2 may have been stripped from the culture when it was sparged with 1 vvm of 100% N_2 gas. When oxygen is present, stripping CO_2 from the culture is not an issue since glycolytic CO_2 is formed.

The presence of cell growth under 2% CO_2, 98% N_2 condition confirmed that the lack of growth under 100% N_2 condition was not due to the toxicity of induction.

Comparing the rate at which glucose was consumed for aerobic and strict anaerobic conditions (Figure 16), the shortage of NAD was evident in the strict anaerobic condition. The glucose utilization rate depends on available NAD, which depends on the amount of oxygen available. As noted by Lin [17], anaerobic cultivation did not promote fast growth rate and resulted in low biomass.

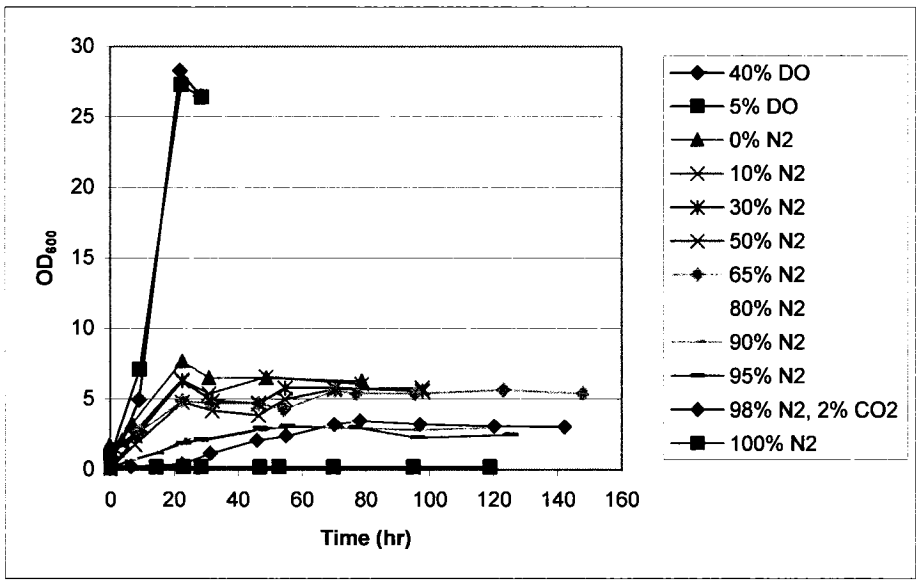

Figure 17. Growth of *E. coli* cultures post inoculation under aerobic, microaerobic, and anaerobic conditions. Cell density measured at optical density of 600 nm.

The growth (cell mass accumulation) of the culture was also dependent on the amount of oxygen available to the cells. At 40% and 5% DO maintained in the bioreactor with increased stir rate, cells favored aerobic catabolic pathway and produced CO_2 and ATPs. The energy from ATP was probably used for cell division and

maintenance, multiplying and preserving cell mass. Most of the carbon supplied by glucose was metabolized and incorporated into cell mass which resulted in OD_{600} above 25 (Figure 17). In comparison, when oxygen delivery was only adjusted in the inflow (no stir rate increase for microaerobic case), a peak cell density of 3-8 OD_{600} was observed. According to Figure 17, approximately a five-fold increase in cell density was obtained in aerobic processes compared to microaerobic processes. Aerobic cultivation resulted in higher cell density as described by Cheng [27] and microaerobic cultivation was successful in restricting the carbon flow to cell mass.

In addition, the rate of cell growth corresponded well with the rate of glucose consumption. Under aerobic process conditions, glucose consumption and cell growth were complete within 24 hrs post inoculation (Figures 16 and 17). In the higher microaerobic range (shown in green), peak cell density and glucose depletion were attained around 30 hrs. The growth lagged for the lower microaerobic range (shown in orange) where the peak cell density was seen after 50 hrs when glucose was used up. This point is also illustrated in Figure 18 which shows both glucose depletion time and the maximum cell density at OD_{600} for all conditions. For most conditions, peak cell density was achieved at the time glucose was depleted. Since the rate of cell growth mirrors the rate of glucose utilization rate, and glucose utilization rate is proportional to oxygen availability, the rate of growth is also correlated with oxygen availability. Slower cell growth was observed with lower oxygen concentration in the medium. Thus, induction at 3.0 OD_{600} for each run was achieved at different times post inoculation.

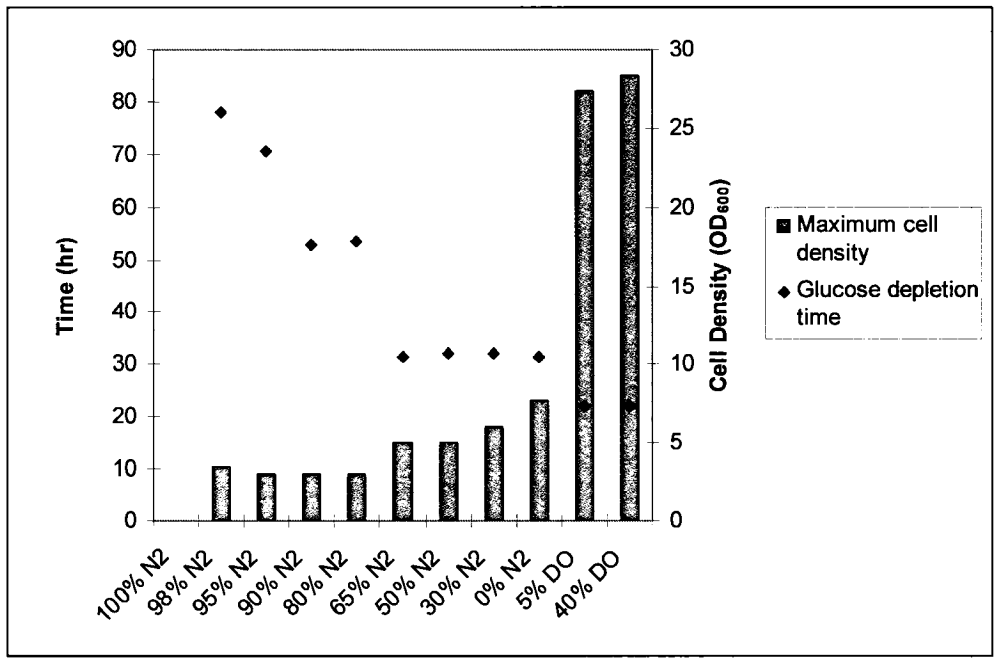

Figure 18. Approximate time of glucose depletion and maximum cell density obtained under aerobic, high microaerobic, low microaerobic, and anaerobic conditions.

5.3 Effect of Aerobic, Microaerobic, and Strict Anaerobic Processes on Organic Acids Production

The generation of reduced fermentation products was expected from microaerobic and anaerobic cultures to sustain redox balance and to generate NAD and ATP as described by Bermejo [24]. With the varying degrees of microaerobicity tested, different carbon distributions among organic acids were also expected.

All anaerobic (fermentative) byproducts, shown in the anaerobic catabolic pathway in Figure 15, were detected and quantified using HPLC. Figures 19 thru 23 show the measured amount of lactate, formate, acetate, ethanol, and succinate, respectively, during the cultivations. Based on the results for each figure, with the exception of Figure 22, five distinct patterns of behavior were evident. The twelve

different conditions tested can be categorized into five groups: 1) aerobic processes (blue), 2) high microaerobic range (green), 3) low microaerobic range (orange), 4) strict anaerobic condition with CO_2 supplementation (pink), and 5) strict anaerobic condition with no CO_2 supplementation (red).

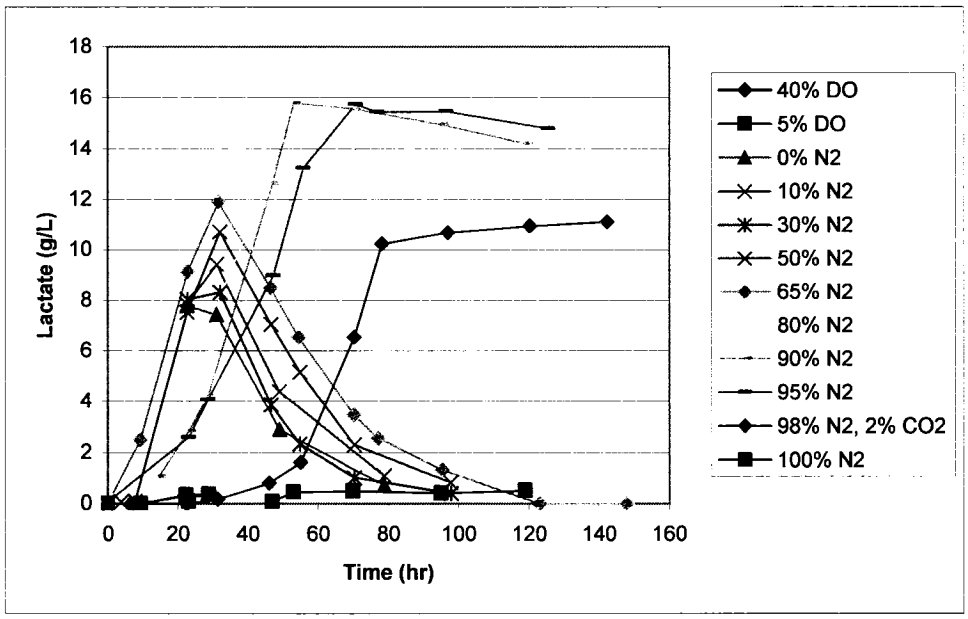

Figure 19. Lactate concentrations detected during aerobic, microaerobic, and anaerobic cultivations.

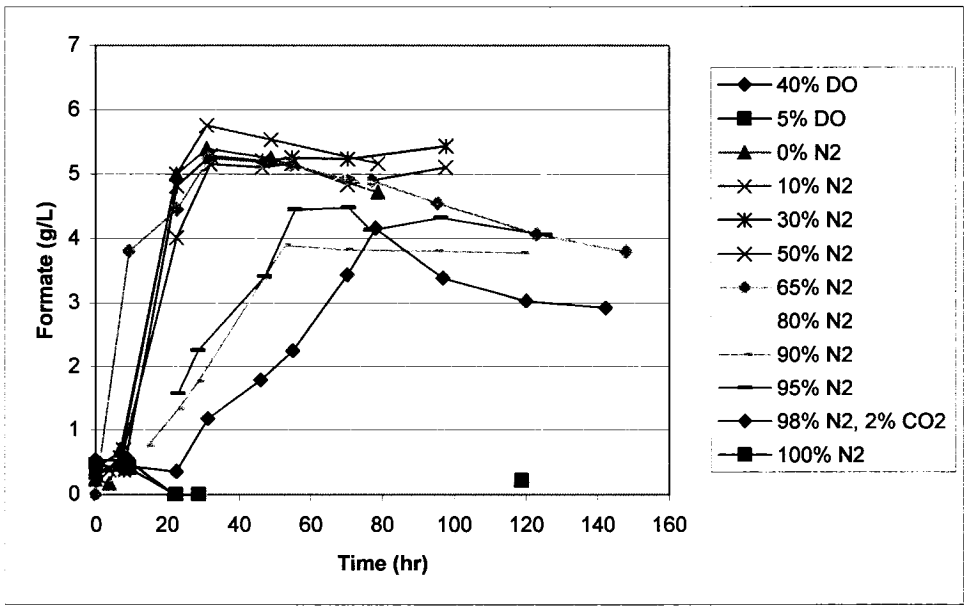

Figure 20. Formate concentrations detected during aerobic, microaerobic, and anaerobic cultivations.

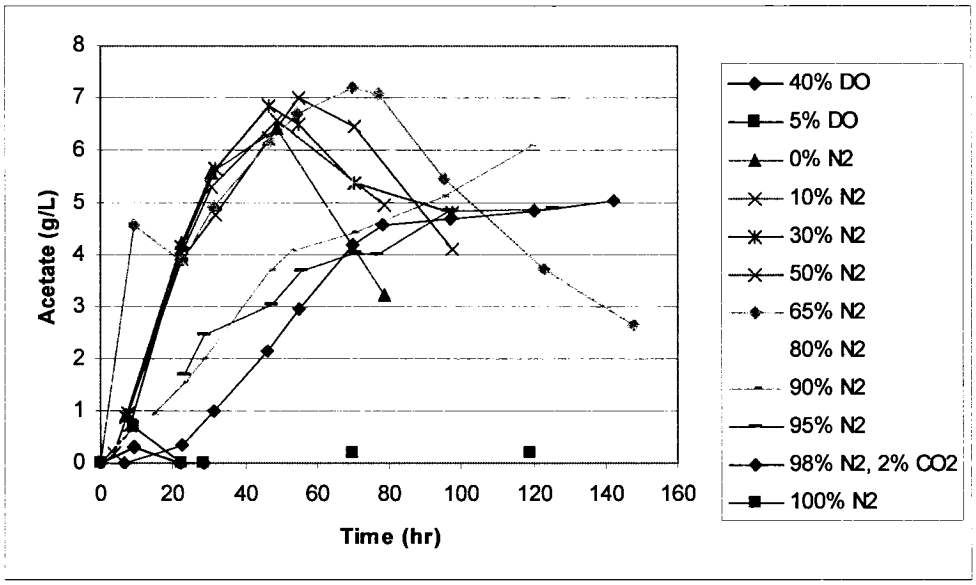

Figure 21. Acetate concentrations detected during aerobic, microaerobic, and anaerobic cultivations.

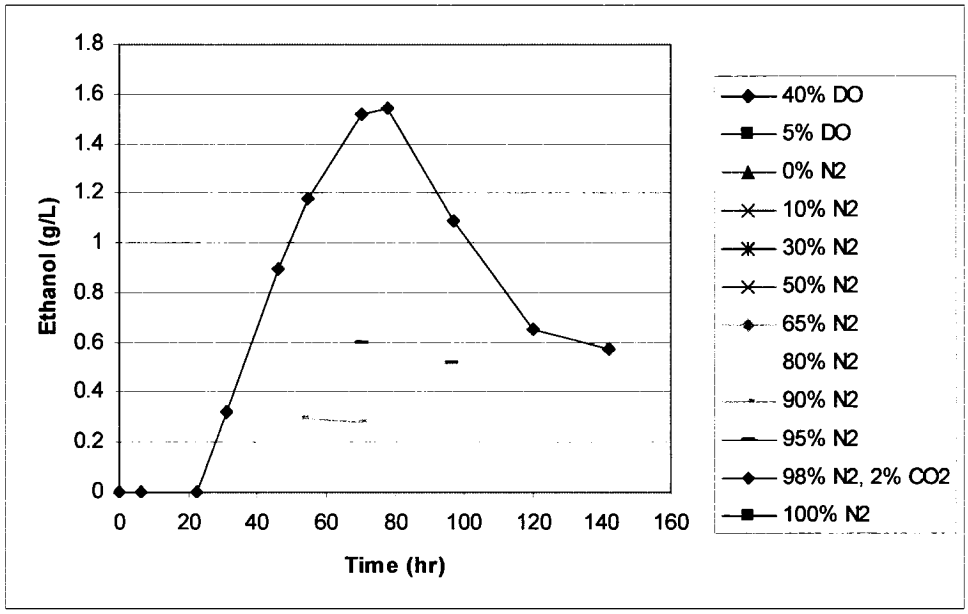

Figure 22. Ethanol concentrations detected during aerobic, microaerobic, and anaerobic cultivations.

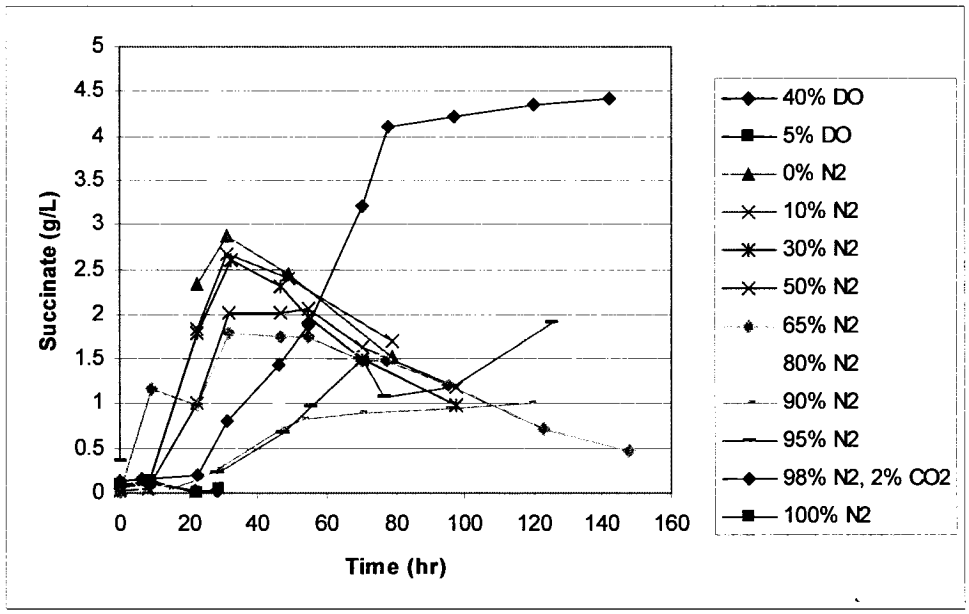

Figure 23. Succinate concentrations detected during aerobic, microaerobic, and anaerobic cultivations.

5.3.1 Aerobic Process

During the aerobic processes, no significant amounts of organic acids were made as shown in Figure 24. A few traces of formate and succinate were detected at the start of the cultivation, possibly carried over from the seed culture. The generation of other acids may be explained by the glucose effect (catabolic repression). In the presence of excess glucose, the synthesis of respiratory enzyme necessary for respiratory sugar metabolism is known to be repressed by excess glucose present in the batched glucose medium, regardless of the high oxygen concentration [22]. The amount of organic acids produced here was insignificant and even the small amount of acetate generated was reconsumed by the cells soon after and depleted by the end of cultivation.

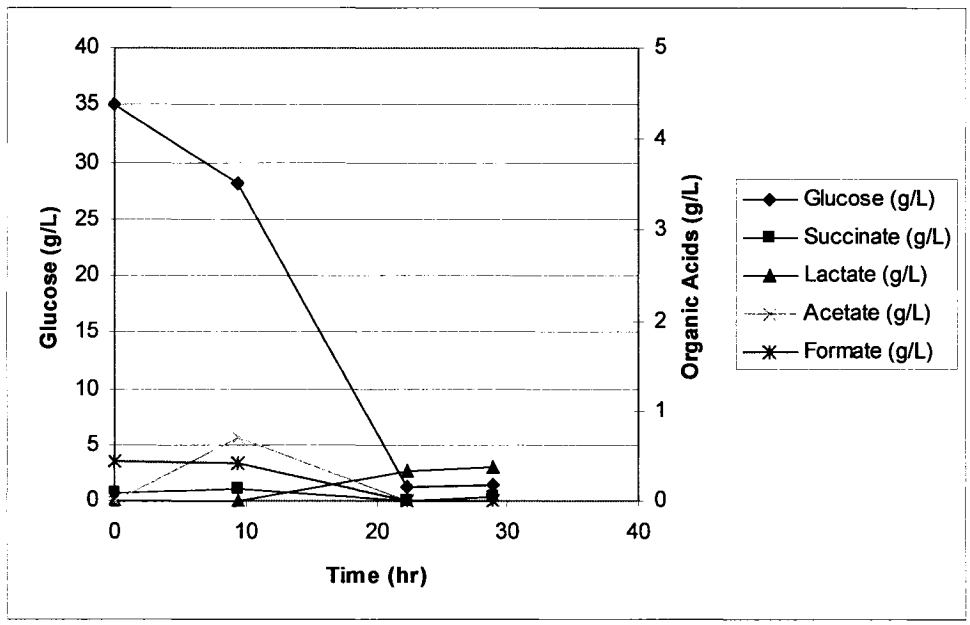

Figure 24. Glucose consumption and organic acids production during 5% DO aerobic process cultivation.

5.3.2 High Microaerobic Operating Range

In the high microaerobic range (0-65% N_2), the maximum lactate concentration reached between 8-12 g/L at 30 hrs after inoculation (Figure 19). The highest formate and succinate production were also attained around that time (Figures 20 and 23). The timing of maximum lactate, formate, and succinate production corresponded to the time of glucose depletion seen in Figure 16. The peak acetate formation followed later at 50-70 hrs with a maximum of 6-7 g/L.

The appearance of lactate in the fermentation culture under high microaerobic operating range suggested that NAD might be limited initially under these conditions. Lactate is one of the first organic acid products generated from pyruvate when NAD, hence oxygen, is most restricted (Figure 15). However, complete disappearance of lactate over time suggested that sufficient amounts of NAD became available to recycle this three carbon molecule back into the catabolic pathway using the reverse reaction. Lactate converted back into pyruvate is decomposed into acetyl-CoA either to make acetate, whose production peaks soon after the disappearance of lactate, or to make mevalonate (Figure 7). Carbon atoms in succinate and acetate were also reconsumed. This reuse of byproducts by the cells in the presence of oxygen was reported by Cheng [27]. The cells feed on glucose initially as a carbon source and once it is depleted, they consume lactate and succinate, followed by acetate, as shown in Figure 25 under high microaerobic conditions. These carbons can be fed into the heterologously expressed mevalonate metabolic pathway.

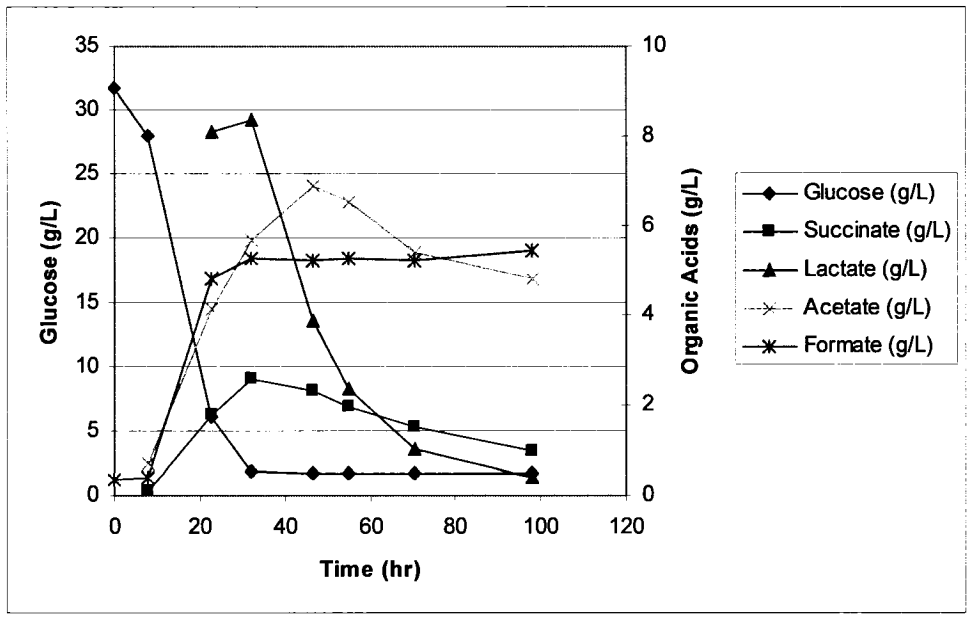

Figure 25. Glucose consumption and organic acids production during 30% N_2, 70% air high microaerobic cultivation.

The only byproduct which seemed to accumulate without reconsumption was formate (Figures 20 and 25). Up to 6 g/L of formate was generated and remained at steady concentration throughout 100-hr cultivation. PFL (pyruvate formate lyase) is responsible for breaking pyruvate into formate and acetyl-CoA when oxygen is restricted (Figure 15). Once the single carbon formate is formed, it is not fed back into the catabolic pathway. Furthermore, formate can be broken down to CO_2 and H_2 by the formate hydrogenlyase complex [44]. However, decomposition of formate was not confirmed. The enzymes appeared to be insensitive to oxygen concentration since formate accumulation occured under most conditions. However, in the 65% N_2 condition with 150-hr cultivation, some decrease in formate concentration was observed. During

longer cultivation formate may have evaporated out from the liquid phase due to its high volatility [45].

5.3.3 Low Microaerobic Operating Range

The oxygen content in the inflow gas was highly restricted for microaerobic conditions between 80% N_2 and 95% N_2. This low microaerobic operating range resulted in the accumulation of most organic acid byproducts including lactate, formate, acetate, and succinate (Figures 19, 20, 21, and 23). The highest amount of organic acid made was 16 g/L of lactate at 50 hrs, which gave lactose yields greater than 50% (wt/wt) from the starting material of 30 g/L of glucose. The higher restriction of oxygen translated into a higher drive to form and accumulate lactate, the first reduced product generated to maintain redox balance, due to the lack of NAD. A peak production of formate and succinate at 50-70 hrs immediately followed peak lactate production, followed by increasing acetate production beyond 70 hrs. Under such restricted oxygen conditions, cells were incapable of reusing the byproducts regardless of the presence of oxygen. What Cheng [27] has reported about the reuse of byproducts by the cells did not apply at highly restricted microaerobic ranges.

As previously discussed, the carbon flow towards organic acids at different steps of the catabolic pathway is determined by oxygen and NAD availability. However, the reason for the formation of organic acids other than lactate at such oxygen restricted condition could be explained by enzyme kinetics. If the turn over rate of the enzyme responsible for converting pyruvate to lactate (LDH, lactate dehydrogenase) did not keep

up with the flow of carbon in the pathway, then products further down the pathway such as acetate and ethanol could be formed subsequently. Because the condition does not provide extra NAD, reduced products remain where they are in the pathway. As an illustration, the glucose consumption and product formation and accumulation of the low microaerobic condition of 95% N_2 and 5% air are shown in Figure 26.

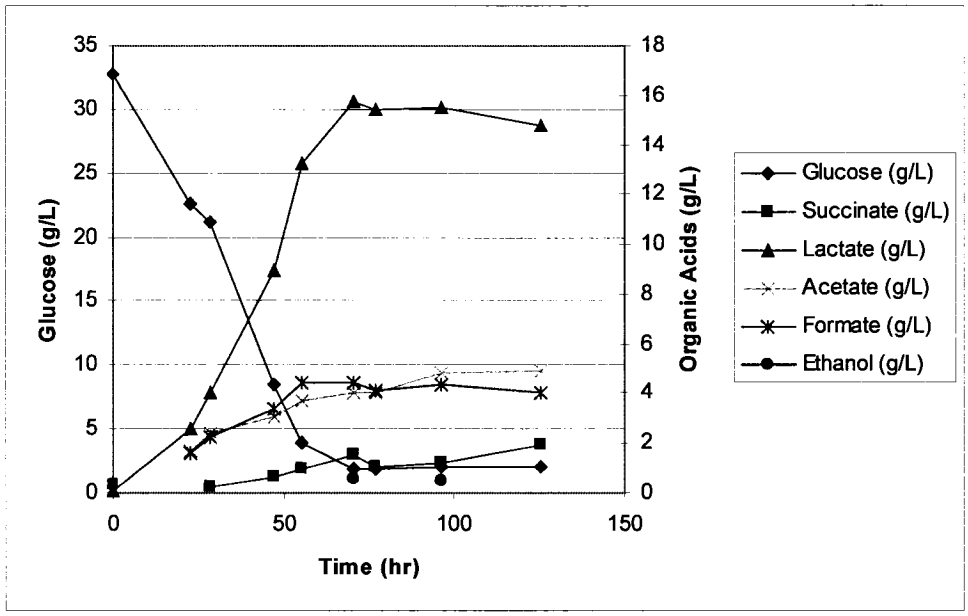

Figure 26. Glucose consumption and organic acids production during 95% N_2, 5% air low microaerobic cultivation.

Ethanol is made to cancel 2 NADH generated in metabolizing ½ mole of glucose in the pathway up to acetyl-CoA, and acetate is made to gain cellular energy in the form of ATP [21]. In the low microaerobic operating range, up to 0.6 g/L of ethanol was detected by the HPLC (Figure 22); however, it seems to have stripped off from the liquid

phase over time due to the high gas flow rate. Ethanol concentration in the off-gas was too low to be detected by the off-gas analyzer.

5.3.4 Strict Anaerobic Condition with CO_2 Supplementation

The strict anaerobic condition with 2% CO_2 supplementation process behaved significantly different from the low microaerobic range process. The highest production of lactate was anticipated under this condition out of all the conditions tested since there was no oxygen supplied. However, the lactate production leveled off at 11 g/L, which was 5 g/L less than the low microaerobic conditions (Figure 19). However, formate and acetate formation were comparable to the low microaerobic conditions (Figures 20 and 21). The deficit of 5 g/L lactate in carbon equivalence was distributed into making 1.5 g/L of ethanol and 4.5 g/L of succinate. Both ethanol and succinate were produced in the highest amount out of all the conditions (Figures 22 and 23). The products of the mixed acid fermentation are shown in Figure 27.

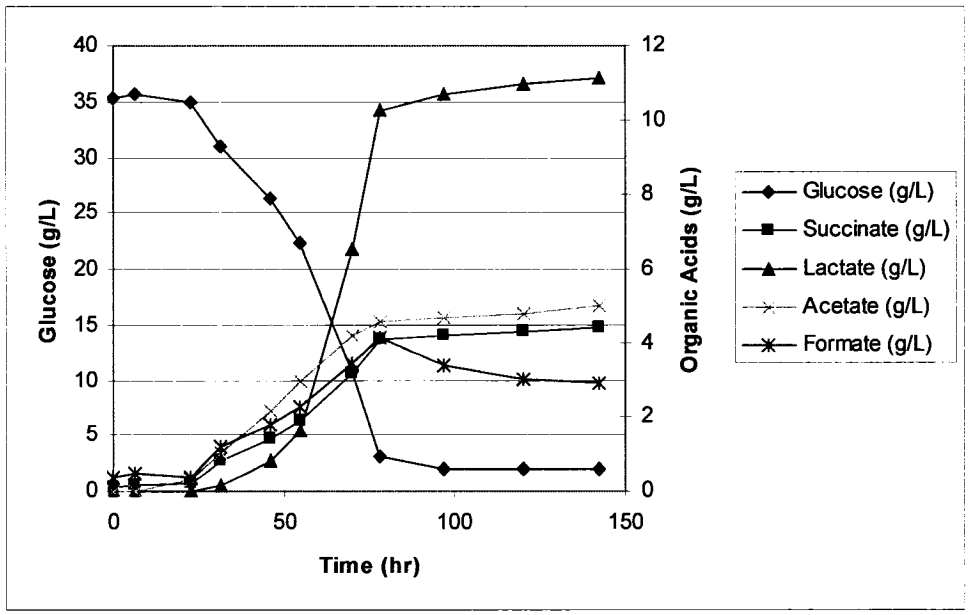

Figure 27. Glucose consumption and organic acids production during strict anaerobic condition of 98% N_2, 2% CO_2 cultivation.

Succinate is one of the components in the TCA cycle and its formation is observed in anaerobic cultivation [17]. When oxygen is most restricted and the glycolytic enzymes that make organic acids become saturated (i.e., LDH and PFL), phosphoenolpyruvate (PEP) and pyruvate are converted to oxaloacetate. From PEP to oxaloacetate, CO_2 is required, which was consistent with the need of CO_2 supplementation for growth under strict anaerobic condition for the mevalonate strain. Under anaerobic catabolism, oxaloacetate in the TCA cycle can be directed into either direction of the cycle with succinate as the end product, illustrated in Figure 28. By favoring the reaction in counter-clock wise direction, cells are able to regenerate NAD.

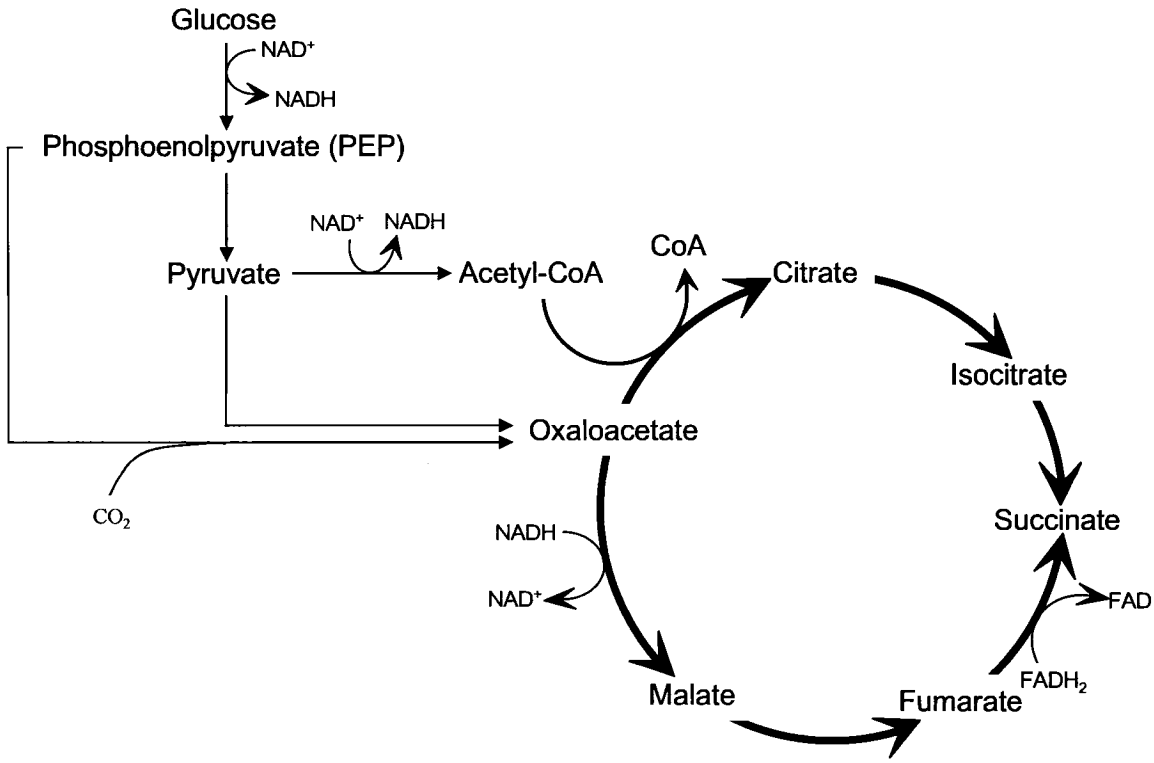

Figure 28. Succinate production from glucose catabolism under anaerobic cultivation.

According to Bermejo [24], one mole each of ethanol and acetate in addition to two moles of formic acid are produced per mole of glucose in *E. coli* in anaerobic, no-growth conditions. In this work, 1.6 g/L of ethanol, 4.5 g/L acetate, and 4 g/L of formate were formed in no-growth conditions at 80 hrs which translate into 35 mM, 75 mM, and 87 mM, of each product respectively. The findings here show approximately 1:2:2 ratios of ethanol, acetate, and formate instead of 1:1:2 in no-growth conditions.

5.3.5 Strict Anaerobic Condition with no CO_2 Supplementation

When no CO_2 was supplied in strict anaerobic condition (100% N_2), batched glucose remained untouched and thus, no cell growth was observed as discussed in Section 5.2. This translated into no noticeable production of fermentative products (Figures 19 through 23). Despite no growth, the culture was induced with IPTG at 47 hrs post inoculation. The appearance of low concentration of lactate after 50 hrs on Figure 19 may be due to the conversion of IPTG, a molecular mimic of allolactose, to lactate. The cells were not responsible for the formation of lactate in this condition.

5.3.6 Base and Acid Addition

Base addition to the cultures was necessary to maintain the pH at 7.0. Ammonium hydroxide was used as a base to compensate for the production of organic acids. The amount of ammonium hydroxide at 9.9 N added into the bioreactor under each condition is shown in Figure 29. Assuming no additional base was fed into the bioreactor via evaporation through the base addition line, one can estimate the amount of organic acid products generated from the amount of base added on a molar basis. The trend of base addition (Figure 29) resembles that of lactate production (Figure 19). At 100% N_2 condition where metabolic activity was zero, slow yet increasing addition of base was observed over time. The formation of lactic acid from IPTG may have caused the shift of pH requiring the addition of the base. Furthermore, the evaporation of ammonium hydroxide out from the medium, due to its high volatility, may also have played a role in the addition of the base while cells were inactive.

The addition of the base stopped when organic acids production was completed. As cells recycle carbons from organic acid products, the culture became more basic, requiring the addition of the acid to maintain the pH at 7.0. Sulfuric acid solution at 5 N was used and its relative addition for all runs is compared in Figure 30. More acid addition was observed under high microaerobic conditions than any other cases because all acidic byproducts except for formate and CO_2 were reconsumed. With almost no organic acids formed during aerobic cultivation, the amount of sulfuric acid addition to the culture was minimal.

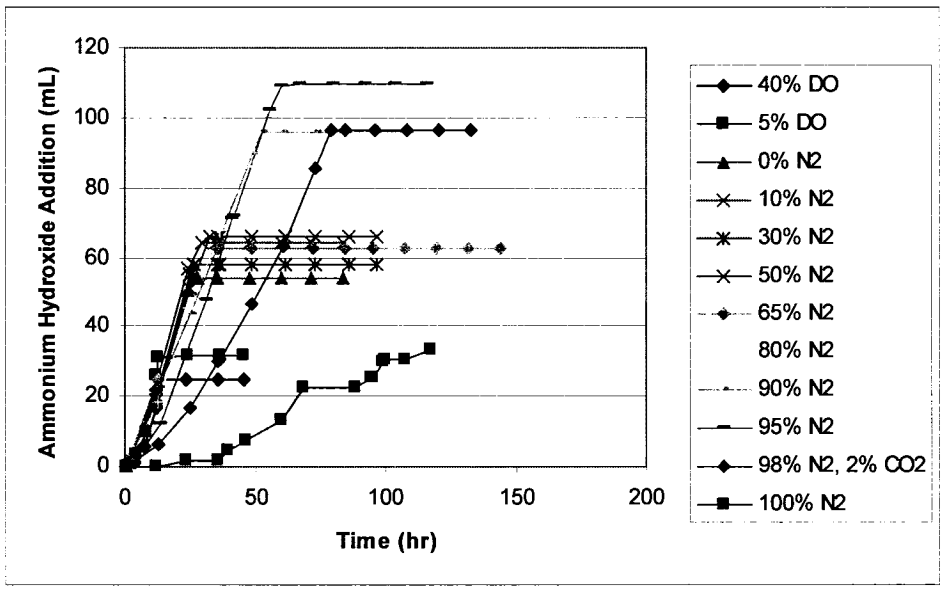

Figure 29. Addition of 9.9 N ammonium hydroxide solutions to the culture during aerobic, microaerobic, and anaerobic cultivations.

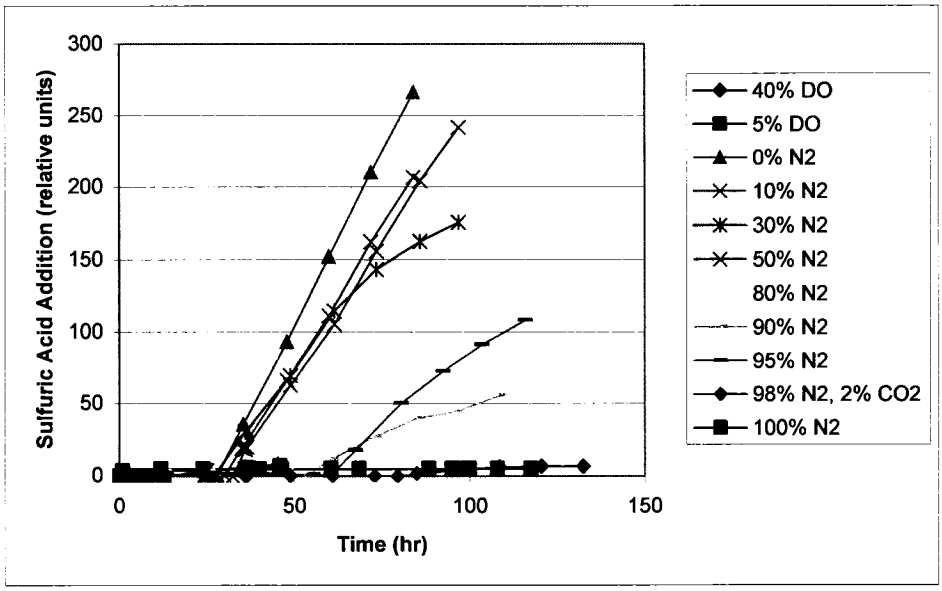

Figure 30. Addition of 5 N sulfuric acid solutions to the culture during aerobic, microaerobic, and anaerobic cultivations.

5.4 Effect of Aerobic, Microaerobic, and Strict Anaerobic Processes on Mevalonate Production, Specific Productivity, and Yields

5.4.1 Mevalonate Production

To make one mole of mevalonate (C_6), it requires 3 moles of acetyl-CoA (C_2x3) made from 1.5 moles of glucose (C_3x3). When most of the carbon is converted into cell mass, as in the case with the aerobic process, not much of carbon is left for the production of mevalonate. Similarly, if the carbon is accumulated in the forms of organic acids due to lack of NAD, as seen in the low microaerobic range, the same can be said about the carbon flow into the mevalonate pathway. Figure 31 shows that both aerobic processes and low microaerobic range resulted in an average of less than 2 g/L mevalonate. The biggest difference between the two conditions was that glucose was exhausted much faster in the aerobic process. Due to this, the peak mevalonate titer for

the aerobic process was achieved much faster, shortly after 20 hrs post inoculation, as oppose to 80 hrs for the low microaerobic range above 90% N_2 condition, shown in Figure 32. Estimating 2 g/L mevalonate for these cases, the yield on glucose was approximately 6.6% (wt/wt) or 8.1% by molar basis.

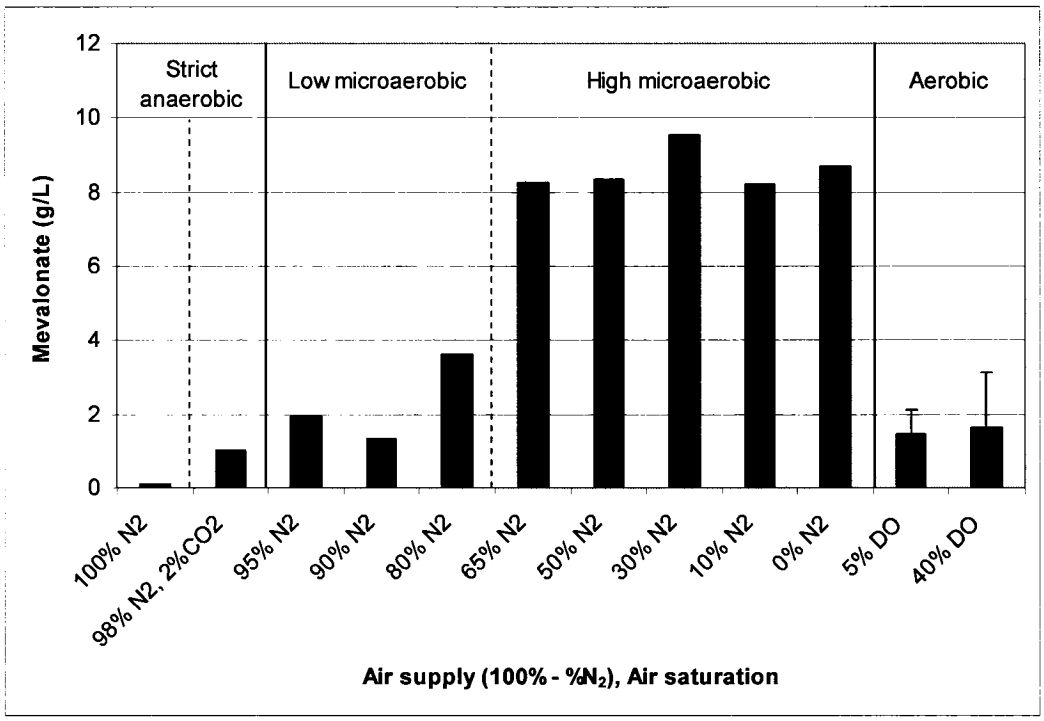

Figure 31. Mevalonate production by 100 hrs under aerobic, high microaerobic, low microaerobic, and anaerobic conditions with and without CO_2 supplementation (right to left). An average of two runs shown with the range in error bars for the aerobic conditions.

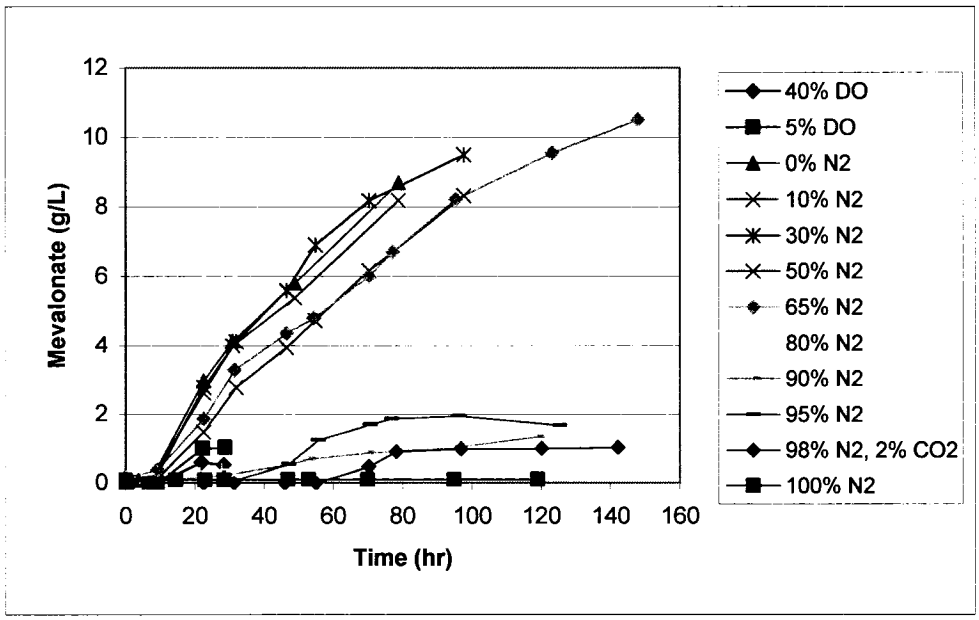

Figure 32. Mevalonate production over time under aerobic, microaerobic, and anaerobic cultivations.

Between 65% and 0% N_2, mevalonate titers were between 8-10 g/L by 100 hrs (Figure 31). The high microaerobic range above 30% N_2 seemed to produce mevalonate slightly faster than 50% or 65% N_2 conditions (Figure 32). At 65% N_2, the highest mevalonate titer attained was above 10 g/L at 150 hrs (Figure 32). The extended cultivation time helped in converting more organic acids byproducts into mevalonate. It was apparent that other cultivation runs had similar potential of making additional mevalonate since more acetate and succinate were present at the end of their cultivation at 100 hrs (Figures 21 and 23). The conversion of 30 g/L of glucose to 10 g/L mevalonate yielded 33.3% conversion by weight and 40.5% by moles. The operating range of 30% to 0% N_2 gave the highest yield of mevalonate in shortest amount of time, illustrated by the highest slope on the production curve (Figure 32). It was evident from

Figure 31 that all operating condition between 65% and 0% N_2 resulted in consistent mevalonate titer above 8 g/L.

The peak mevalonate production was significantly reduced from above 8 g/L at 65% N_2 to 3.5 g/L at 80% N_2 condition (Figure 31). Because the results for growth, glucose consumption, and organic acids production at 80% N_2 condition traced nicely with the results from low microaerobic conditions below 80% N_2, in addition to the steady concentration of organic acids over time, it can be assumed that the critical ratio of NADH to NAD to generate maximum mevalonate (i.e., convert organic acids to mevalonate) lies between the 80% and 65% N_2 conditions.

The production of 1 g/L of mevalonate under strict anaerobic condition with CO_2 supplementation (Figure 31) can be attributed to PFL activity that allowed acetyl-CoA formation during anaerobic condition (Figure 15). Although the titer is not spectacular, the mevalonate productivity per cell comes close to that of the high microaerobic conditions shown in Figure 34. The calculation of specific productivity is discussed in Section 5.4.2.

The trace amount of mevalonate detected at 100% N_2 condition (Figure 31) under no cell growth (Figure 17) may be carried over from the seed culture used as an inoculum. During the aerated seed cultivation, no IPTG was added for induction; however, the strain is known to weakly express the top mevalonate pathway without induction and produce low concentration of mevalonate.

The relationship of mevalonate production and oxygen concentration can be derived from Figure 31 and is shown in Figure 33. Although Figure 31 is plotted using

the data by 100 hrs, the shape of the curve on Figure 33 is also valid at the end of the cultivation. Comparing Figure 33 to Figure 8 (b) postulated as a hypothesis in Section 3.1, the mevalonate production from the experimental data showed that no minimum threshold of oxygen feed rate was required for mevalonate production. In addition, a wide operating range of oxygen concentration, corresponding to the plateau on Figure 33, is available for maximizing the yield. This attribute becomes an advantage when the process is scaled up since aeration and oxygen availability become variable due to deficient mixing [21,35]. It may be possible to reproduce this 1-L process in a large scale vessel when such a wide operation range is available for achieving the maximum yield.

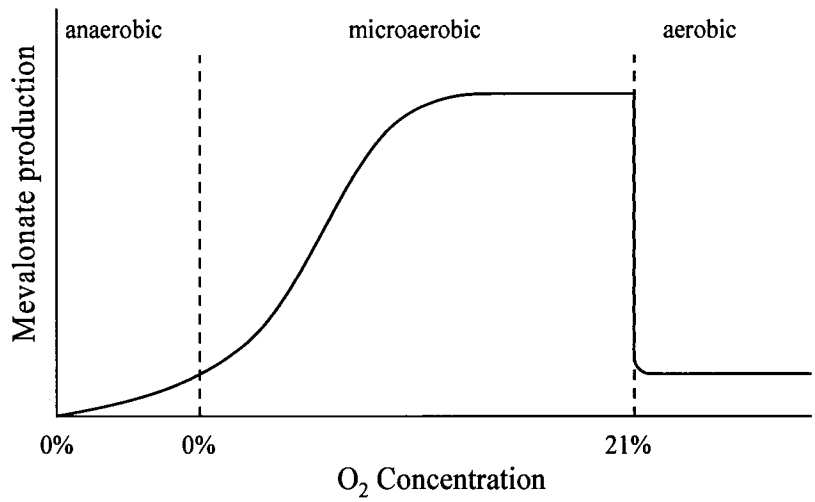

Figure 33. Mevalonate production as a function of oxygen concentration based on experimental data estimated from Figure 31.

In Figure 8 (b), the decrease in mevalonate production in the aerobic process due to the generation of high biomass was not considered. From the experimental data, it is evident that carbon spent on building biomass cannot contribute to making mevalonate.

At high cell densities, low mevalonate production was observed. The two aerobic cultivation conditions repeated twice, shown in Figure 31 with error bars reflecting the range, emphasizes this point. The higher end of the error bar in each case represents the mevalonate titer from a cultivation that was successfully induced at OD_{600} of approximately 3.0. The lower end of the bar was the titer from the late induction process where the induction OD was slightly above 7.0. Once the carbon goes to biomass, it cannot be recycled back into metabolites; hence, no additional mevalonate can be made.

5.4.2 Specific Productivity

Specific productivity of mevalonate for each run was calculated using Equation 5, where x is mevalonate titer in mg per L, and t is time post inoculation in hrs:

$$Specific\ productivity\ (mg\ mevalonate / L / hr / OD) = \frac{x_2 - x_1}{average\ (OD_1, OD_2) * (t_2 - t_1)}$$

Equation 5

The two time points from each run where mevalonate production is linear, on Figure 32, were used for the calculation. The same Δt was not applied for all runs. Figure 34 shows the results both in mg mevalonate/L/hr/OD and mg mevalonate/gram dry cell weight (DCW)/day. This analysis is important because it measures how fast mevalonate was being produced on a per cell basis, as well as the ratio of product to cell mass. As expected, the ratio was lower at aerobic conditions (also see Section 5.4.3). Under most microaerobic conditions, the values were consistent between 15 and 20 mg/L/hr/OD. The highest specific productivity was achieved with 80% N_2 at greater than 25 mg/L/hr/OD. This process, however, was not favorable over high microaerobic processes since a total

of more than 25 g/L of organic acids were generated from 30 g/L of glucose and the organic acids were not recycled back into the pathway.

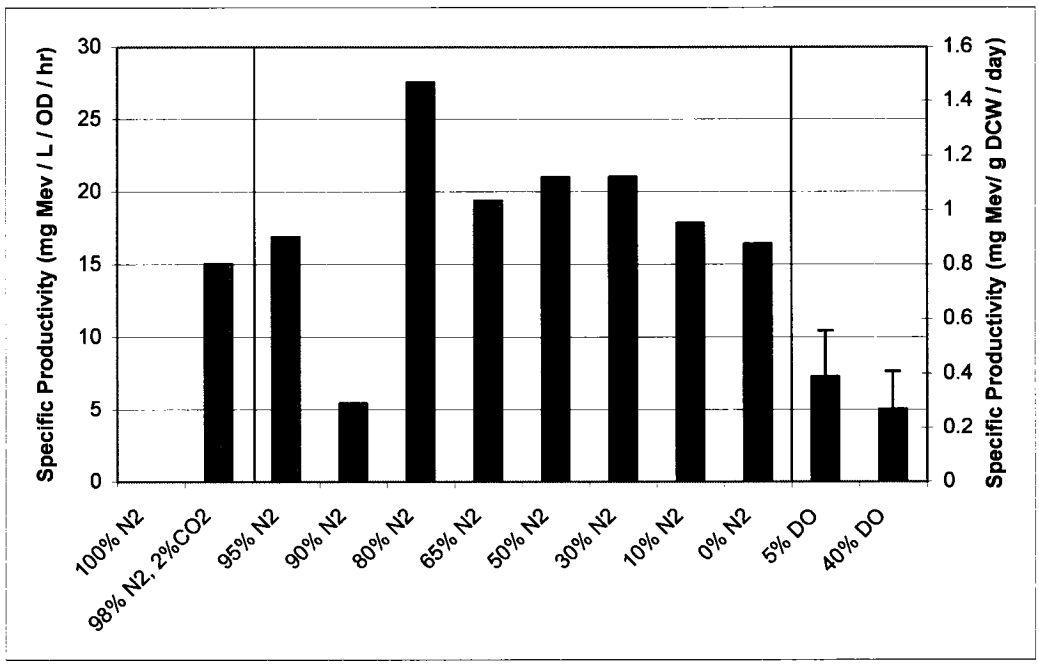

Figure 34. Specific productivity of mevalonate during linear production period under aerobic, microaerobic, and anaerobic cultivations.

5.4.3 Yields and Carbon Products Distribution

Three types of yields were assessed from each run including 1) mevalonate yield on glucose ($Y_{P/S}$, product/substrate), 2) growth yield on glucose ($Y_{X/S}$, biomass/substrate), and 3) mevalonate yield on biomass ($Y_{P/X}$). The corresponding equations are shown in Equations 6 (a), (b), and (c), respectively, and all calculations were done on a weight to weight basis. The highest mevalonate titer time point was selected for all of the runs. For $Y_{P/S}$ and $Y_{X/S}$, the coefficients were defined based on the consumption of glucose, and thus carry a negative sign in the Equations 6 (a) and (b).

$$Y_{P/S} = -\frac{\Delta P}{\Delta S} \qquad \text{Equation 6 (a)}$$

$$Y_{X/S} = -\frac{\Delta X}{\Delta S} \qquad \text{Equation 6 (b)}$$

$$Y_{P/X} = \frac{\Delta P}{\Delta X} \qquad \text{Equation 6 (c)}$$

The mevalonate yields and biomass yields on glucose are shown in Figure 35. The mevalonate yields showed something like a bell-shaped distribution along the oxygen delivery scale. The highest yield was 0.35 or 35% conversion of glucose to mevalonate for the 65% N_2 condition, which was due to the extended cultivation time. But yields above 0.27 were seen consistently among the high microaerobic range processes. At both ends of the curve, the yields were significantly lower. If operated on the left range of the curve, the glucose was converted into organic acids; if operated on the right side of the curve, glucose was used to generate biomass. The growth yields on glucose displayed a different pattern along the oxygen delivery scale. They showed a step-wise increase according to the oxygen delivery rate (Figure 35). In the low microaerobic conditions, the growth yields were below 0.05 or 5% conversion of glucose to biomass. In the high microaerobic range, yields were at 0.08, and in the aerobic range, they were above 0.35. A huge jump in the growth yields between the microaerobic ranges and the aerobic ranges emphasizes the big gap between the two on the oxygen delivery scale and, again, the inefficient use of glucose under aerobic conditions.

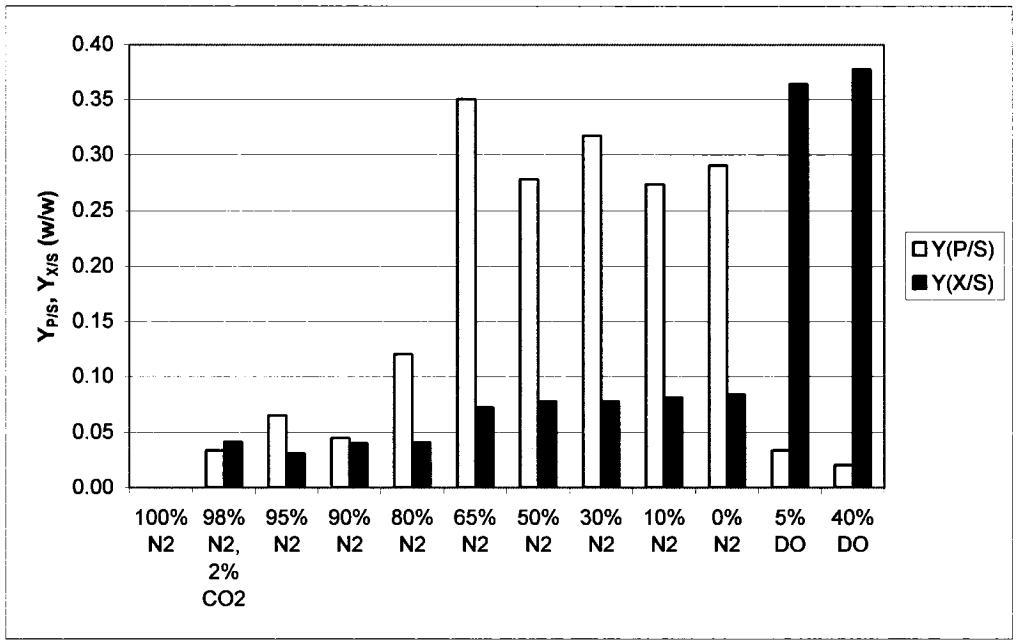

Figure 35. Mevalonate ($Y_{P/S}$) and biomass ($Y_{X/S}$) yields on glucose over aerobic, microaerobic, and anaerobic ranges.

Figure 36 shows the mevalonate yield on biomass. Here, all microaerobic conditions produced more mevalonate per cell mass than the aerobic conditions. Specifically, 65% to 0% N_2 range consistently gave the highest yield.

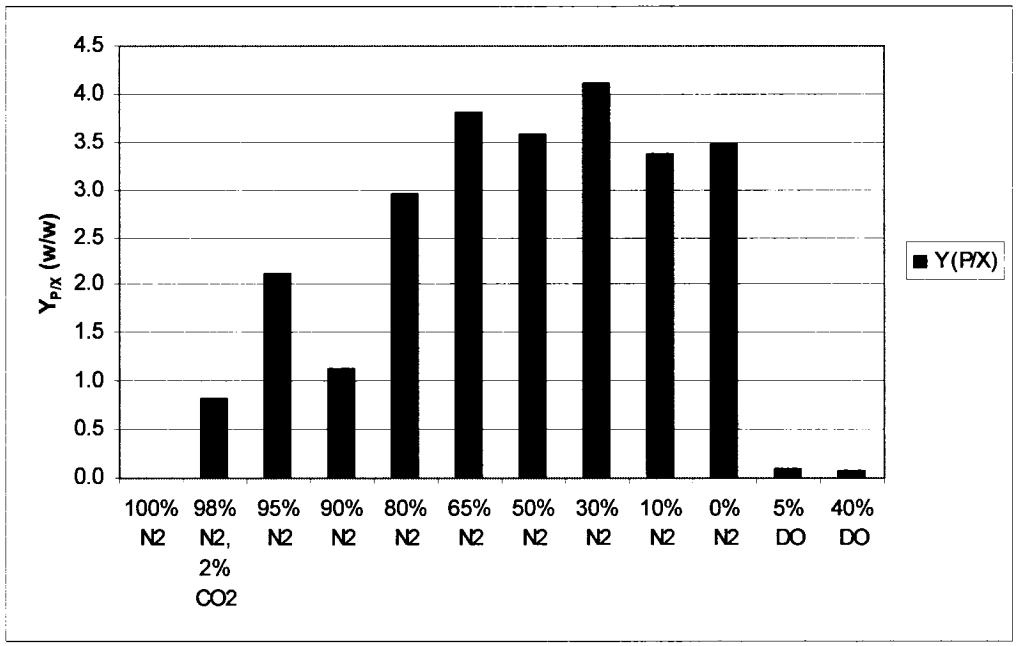

Figure 36. Mevalonate yield on biomass ($Y_{P/X}$) over aerobic, microaerobic, and anaerobic ranges.

The high microaerobic range (0-65% N_2), was the best condition for the strain to attain highest yield of mevalonate on glucose. The product distribution from each oxygen operating range on molar carbon basis is shown in Figure 37 (a) thru (c). At 40% DO cultivation, more than half of the carbon was converted into CO_2 as a result of complete aerobic respiratory catabolism of glucose (Figure 37 (a)). Additionally, more than 40% was transformed into cell mass which left 2% of the carbon available for mevalonate production. If insufficient amount of oxygen was supplied, such as conditions above 80% N_2, then approximately 70% of the carbon was converted into organic acids making it unavailable for the mevalonate pathway (Figure 37 (b)). In the high microaerobic operating range, the optimal carbon distribution was found. The

majority of the carbon was used for mevalonate production at 65% N_2 condition (Figure 37 (c)).

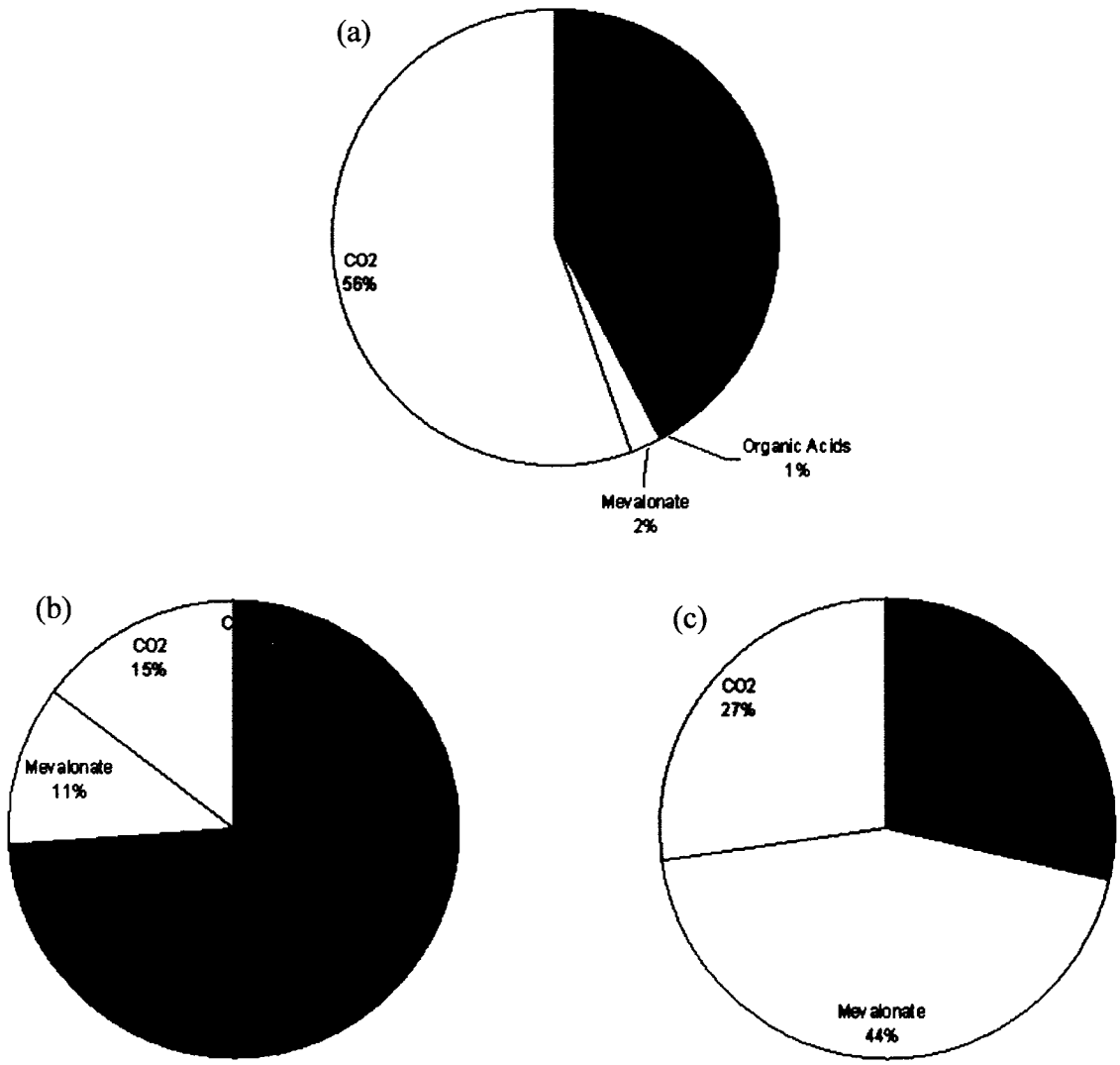

Figure 37. Approximate carbon products distribution at the end of cultivation found at (a) 40% DO, (b) 80% N_2, and (c) 65% N_2 conditions, calculated in percent mole carbon.

5.5 Results on Oxygen Uptake Rate (OUR), CO_2 Evolution Rate (CER), and Respiratory Quotient (RQ)

OUR data collected from the off-gas mass spectrometer suggested that cellular consumption of oxygen depended on the supply of oxygen. On Figure 38, both aerobic conditions reached an OUR close to 1.5 mmol/L/min oxygen at their maximum. The microaerobic and anaerobic conditions remained below 0.25 mmol/L/min OUR and the rates were constant throughout the cultivation. Each rate was proprotional to the amount of oxygen supplied to the culture. The spiking OUR for the aerobic runs and the constant OUR for the microaerobic runs reflect the stir rate profile from Figure 14. The OUR was the result of how much oxygen was supplied into the reactor and how much of it was transferred into the liquid phase.

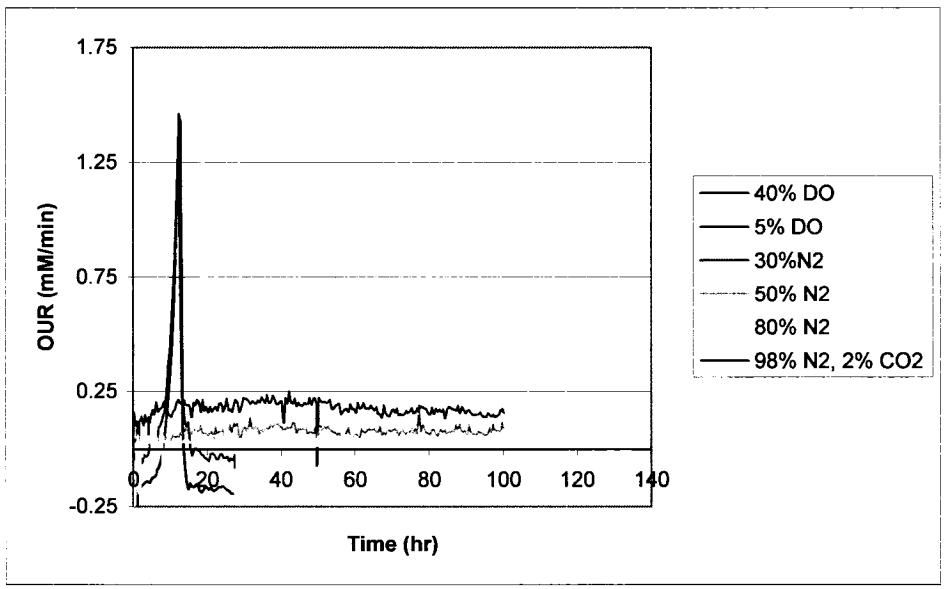

Figure 38. Oxygen uptake rate (mmol/L/min) measured during aerobic, microaerobic, and anaerobic cultivations.

The CO_2 evolution rate was measured from the off-gas. The only detectable CO_2 measurement captured by the instrument was from the aerobic cultivation, where the TCA cycle was continuously active while carbon was available. The CER for aerobic cultivation (Figure 39) was directly proportional to OUR (Figure 38) as expected.

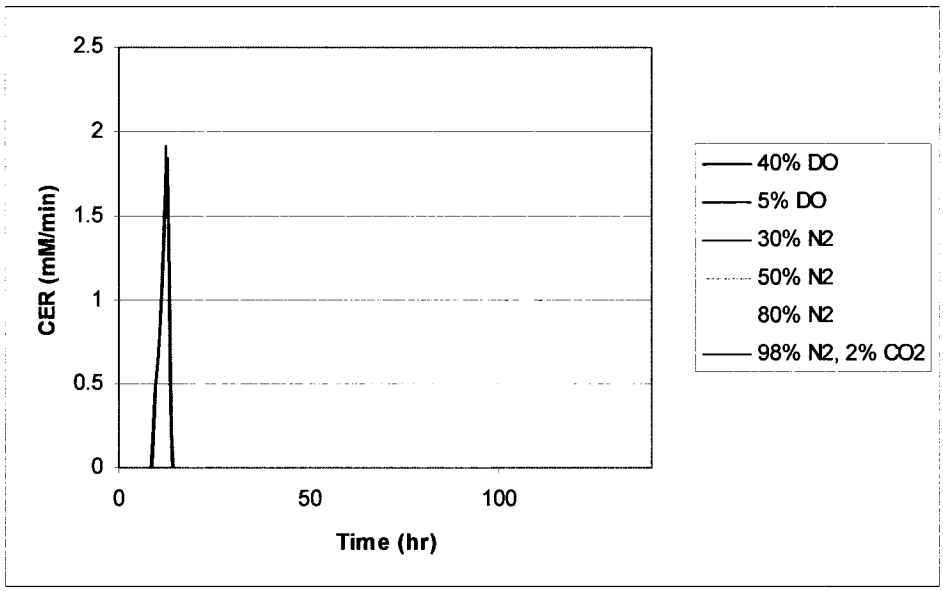

Figure 39. Carbon dioxide evolution rate (mmol/L/min) measured during aerobic, microaerobic, and anaerobic cultivations. Lower CER detection limit at 0.48 mmol/L/min.

Respiratory quotient (RQ) is the ratio of CER to OUR which gives information about the source of energy cells are using. When CER matches OUR exactly (RQ=1), glucose is being metabolized as shown from the balanced chemical reaction in Equation 7, where n=6 for glucose [46]:

$$C_nH_{2n}O_n + nO_2 \rightarrow nCO_2 + nH_2O \qquad \text{Equation 7}$$

One to one stoichiometry of carbon dioxide to oxygen explains the RQ value of one for glucose metabolism. Calculating the RQ for aerobic cultivations from Figures 38 and 39, the ratio is equal to one with the adjustment of the OUR baseline.

No data on RQ was available for the microaerobic cultivations because CER was below the detection limit on the off-gas analyzer for these processes. However, by applying the same concept as Equation 7, the theoretical RQ can be estimated for the cell's metabolism of fermentation byproducts under microaerobic conditions. Lactate ($C_3H_6O_3$) with n=3 has the same RQ as glucose. Acetate ($C_2H_3O_2$) and succinate ($C_4H_6O_4$), on the other hand, have a RQ slightly above 1.0 at 1.14, and ethanol (C_2H_5OH) has a RQ of 1.5, based on the stoichiometry.

5.6 Validation of HPLC Method

The HPLC method developed was successful in detecting and quantifying the amount of glucose, mevalonate, and byproducts. Data collected from RI detector was used for determination of glucose, ethanol, and organic acids concentrations. Both RI and UV were useful in quantifying mevalonate. A chromatogram of a prepared standard solution containing all compounds at 2.5 g/L concentration is shown in Figure 40 (a) and (b) with their respective retention times. Individual peaks were well resolved without tailing. However, with this method, glucose co-eluted with phosphate salts contained in the medium which inflated the peak area for glucose measurement. The starting glucose concentration of 30 g/L was measured between 30 g/L and 35 g/L as seen in Figure 16 (Section 5.2), and zero glucose corresponded to 2 g/L. Straight lines across 2 g/L on Figure 16 indicate depletion of glucose in the culture. The closed carbon balance also

validated the HPLC method (see Section 5.7). If the analysis over or undercounted analytes, then the balance would not be close to 100% for all samples.

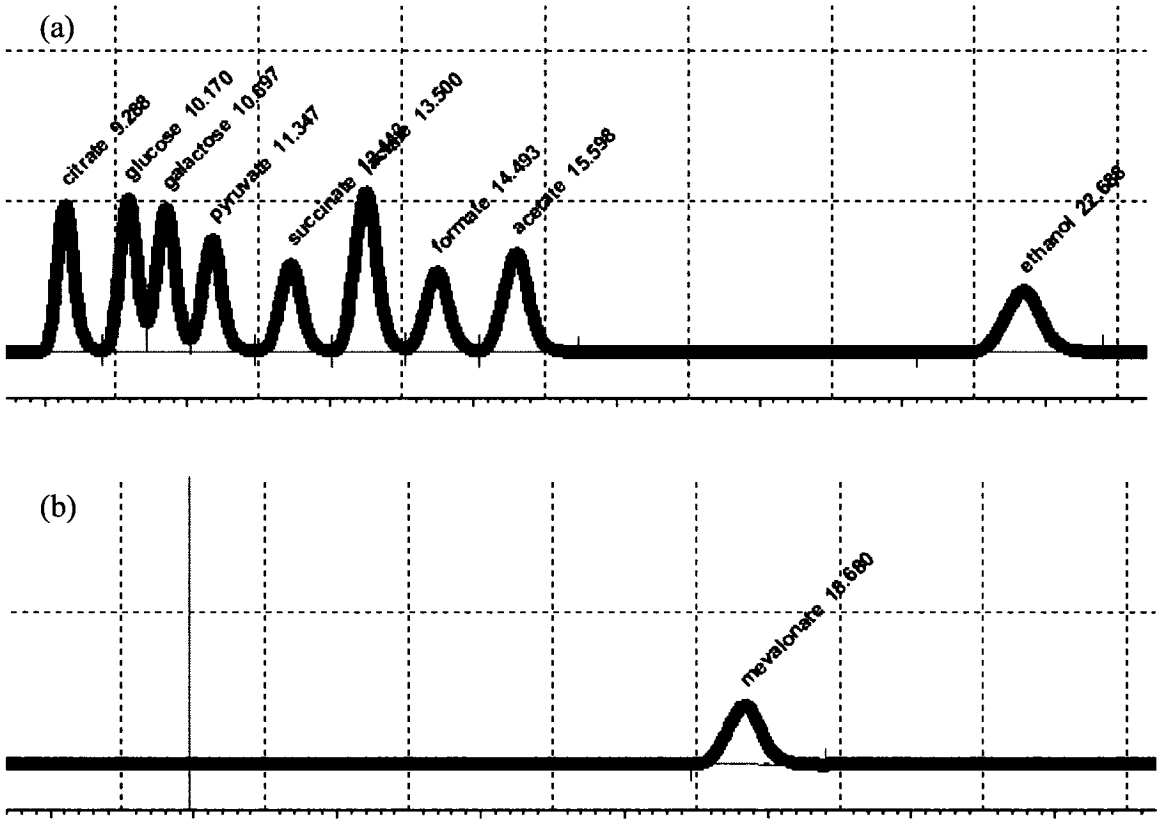

Figure 40. HPLC chromatograms of standard solutions containing (a) organic acids and (b) mevalonate. Retention times of RI detector indicated next to each peak. Succinate and lactate eluted at 12.4 min and 13.5 min, respectively, shown in (a).

5.7 Carbon Balance

The carbon balance calculation was performed to confirm that the total amount of carbon distributed into different products at any given time during the batch cultivation was the same as the starting carbon concentration. The cell mass measured in OD units was translated into DCW (g/L) using the correlation graph on Figure 41. DCW was then converted into molar (M) concentration to fit into Equation 4 from Section 4.2.5.

Metabolites quantified by HPLC were used in the calculation. The glucose concentration was estimated by subtracting the PO_4 peak area detected when glucose was depleted as discussed in Section 5.6. The same PO_4 peak area was subtracted from all time points since PO_4 was supplied in excess and not used in significant amount from the medium. The initial and final PO_4 concentrations in the cultures remained unchanged as measured by Nova Bioanalyzer.

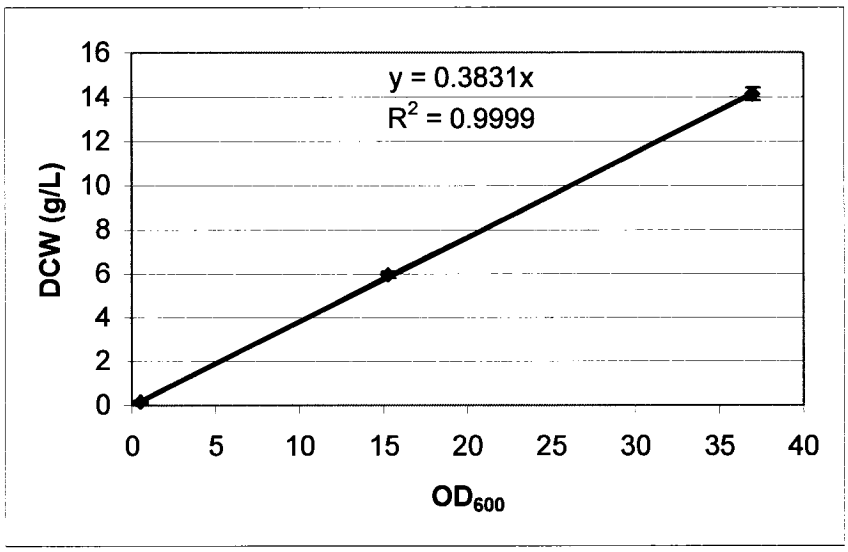

Figure 41. Correlation of cell density (measured at optical density at 600 nm) to dry cell weight. An average of two data points shown with the range in error bars.

The CO_2 was the only product containing carbon that required an off-gas analyzer for quantification. The lower detection limit of the instrument at 0.48 mM per minute allowed measurements above the limit, and any concentration below the limit measured zero. CO_2 generation in the microaerobic processes was below the detection limit. To account for the carbon in CO_2 in these cases, theoretical CO_2 generation was calculated from products or intermediates formed via glycolysis or the TCA pathway: one mole of

CO_2 is generated per mole of acetate, and 3 moles of CO_2 are generated per mole of mevalonate since mevalonate is derived from 3 moles of acetyl-CoA.

Ethanol was quantified via HPLC from a broth sample and the concentration was confirmed by the YSI analyzer. However, due to its high volatility, some may have evaporated out from the liquid phase. The off-gas detection did not detect ethanol in any of the conditions tested. If ethanol was stripped out of the bioreactor during the fermentation, the concentration was too low to be detected by the off-gas analyzer.

The ratio of input to output carbon determined from the carbon balance was used to express carbon recovery (%). Figure 42 illustrates the results for all conditions. Greater than 100% recovery at earlier time points is attributed to the inflated peak area of the glucose from the analytical method. The percent recovery improved over time as glucose became depleted in the cultivation. All data present a carbon balance of 102.7% ± 7.6% standard deviation beyond 20 hrs.

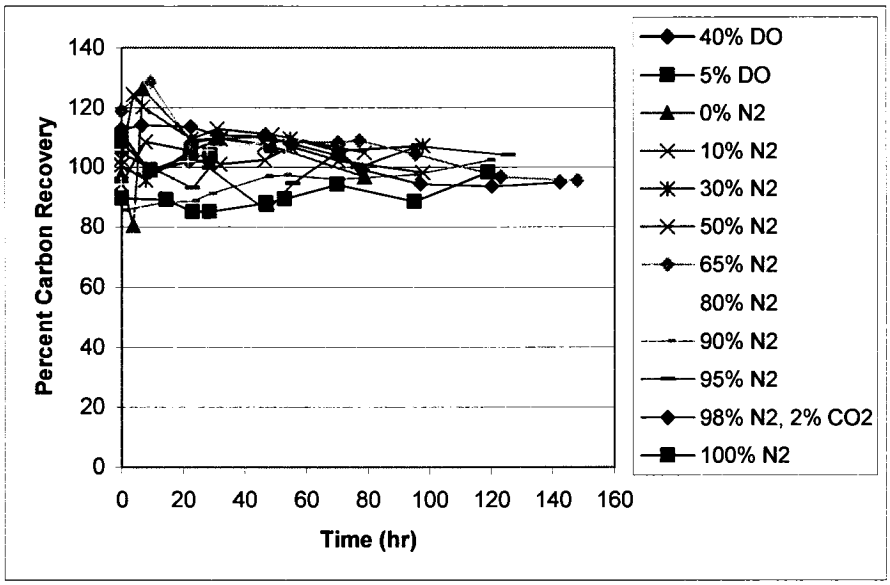

Figure 42. Percent carbon recovery for cultivations under aerobic, microaerobic, and strict anaerobic processes.

5.8 $pO_{0.5}$ Values

Becker carefully studied the $pO_{0.5}$ values for each anaerobic product from *E. coli* batch oxystat cultivations where the value indicated the switch from aerobic to anaerobic respiration. While his study screened different DO concentrations, this work tested different oxygen supplies. If the concept of $pO_{0.5}$ is transferable to O_2 supply as a measure of oxygen, a similar plot to Figure 4 (Section 2.2.3) could be constructed from the results of this work. Figure 43 shows such plot where fermentation products measured at OD_{600} of 3.0 from anaerobic and microaerobic cultivations are graphed against oxygen supply, converted from percent to millibar. With the exception of lactate, one can see the oxygen supply required to reduce each anaerobic product by one-half the maximum synthesis of the products. Both succinate and ethanol require very little oxygen to reduce their concentration by half. Meanwhile, formate and acetate may

require up to 130 millibar of oxygen, equivalent to 40% air, 60% N_2 condition, to switch from anaerobic to aerobic state. Becker's results and Figure 43 support the idea that the synthesis of the alternative products and pathways is regulated in response to oxygen, an electron acceptor [30].

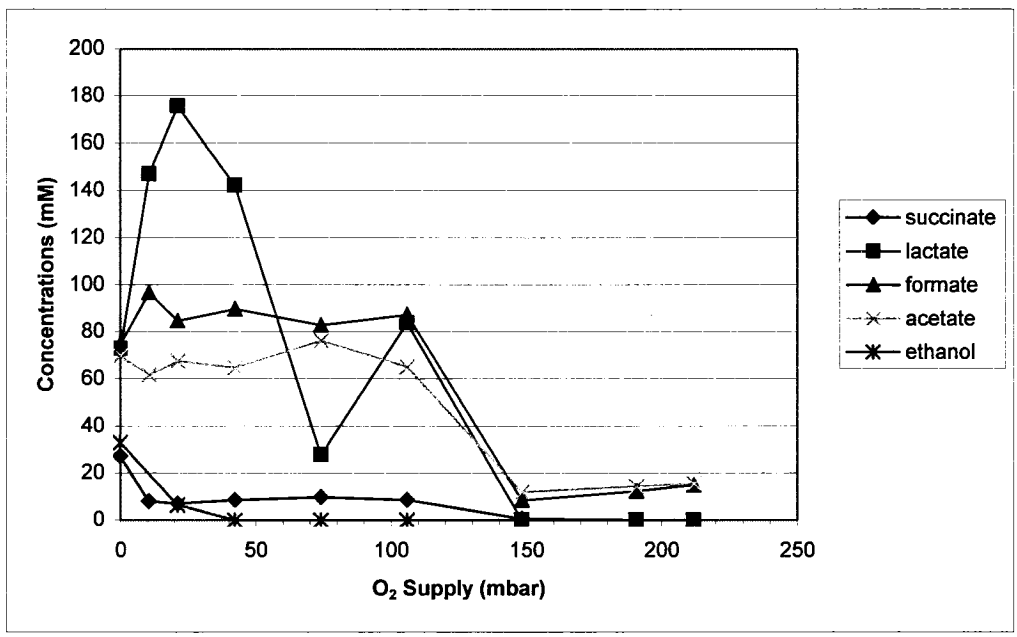

Figure 43. Fermentation products in the supernatants of *E. coli* as a function of O_2 supply during anaerobic and microaerobic cultivations (98% N_2 to 0% N_2 conditions). Products measured at OD_{600} = 3.0.

5.9 100% Aerobiosis

Alexeeva [21] has assigned a parameter called aerobiosis to show differences in cell response among the low oxygen supply range where the DOC cannot be measured. The microaerobic range was thus defined between 0 and 100% aerobiosis. At 100% aerobiosis, complete aerobic behavior was assumed with only CO_2 as the end product containing carbon. Because the strain used for this work harbored the non-native top half

of the mevalonate pathway on a plasmid, the end product of the cultivation consisted of CO_2 and mevalonate, aside from cell mass, under fully aerobic condition of 40% DO.

The CO_2 generation and mevalonate production were the same in the 5% DO process as the 40% DO process (Figures 39 and 31) suggesting that 5% DO was also completely aerobic.

To determine 100% aerobiosis, all conditions tested were evaluated for their product compositions and compared to the aerobic products. An inlet gas supply of 100% air (0% N_2, constant stir rate) was not enough to match a complete aerobic response. The byproducts produced shown in Figures 19 through 23 including lactate, formate, succinate, and acetate suggest the process is still microaerobic. If, however, the amount of time it took to convert all the byproducts into CO_2 and mevalonate was not a factor, then many microaerobic conditions tested would generate aerobic products given enough time. Under such conditions, the level of mevalonate production relies on how much glucose is available to make mevalonate, instead of making additional biomass, which is dependent on the concentration of oxygen available. Thus, no microaerobic condition will give the same product ratio as the aerobic process.

In batch cultivation, 100% air supply at constant stir rate did not achieve complete aerobic response, while at 5% DO-stat (i.e., oxystat) cultivation only the respiratory products were formed. The DO range between 0% and 5% were not tested due to difficulty in controlling low DO set point with a narrow dead band. Because the amount of oxygen availability at 5% DO was exponentially higher, owing to increased stir rate (Figures 14 and 38), than the next highest oxygen supply at 100% air with constant stir

rate, the scale of aerobiosis that Alexeeva had defined for continuous cultures does not seem to apply for batch cultivations. Alexeeva plotted the changes in the specific rate of respiration over increasing percentage of oxygen in the inflowing gas shown in Figure 3 (a) from Section 2.1. Figure 3 (a) shows 100% aerobiosis attained at 14% air in the inflowing gas for continuous cultures. Under batch cultivations, 100% air was insufficient to achieve 100% aerobiosis. Therefore, 100% aerobiosis does not lie on the same linear scale as it did in the continuous cultivations.

5.10 Correlation Between Dissolved Oxygen and Redox Potential Measurements

In addition to the DO probe, a redox probe was incorporated to measure oxidation-reduction potentials in the culture. The advantages of using the redox probe were discussed by Shibai and Dahod [31,32]: 1) At 0% DO or below, the redox probe can detect changes in oxygen availability where DO probe is not applicable, 2) the redox probe measures oxidation state of all species in the culture other than molecular oxygen, 3) the redox measurements give useful information regarding the changes in cell's respiration and activity, and 4) the construction of a redox probe offers more reliable signals than DO probes.

The DO and redox responses observed by Dahod in penicillin fermentation (Figure 5) illustrated the close relationship between the two measurements. Both displayed similar positive responses when oxygen availability was affected by increases in airflow or pressure. This was somewhat true for the mevalonate fermentation. During the first 20 hours of the cultivation while glucose was consumed, the DO and the redox measurements both showed decreasing responses due to the high consumption of oxygen

from cell respiration, as shown in Figure 44. The redox probe, however, outperformed the DO probe by successfully differentiating between the three conditions with air supplied at 40% DO, 10% N_2, and 50% N_2 during this period. The highest oxidation-reduction potential measurement was captured at 40% DO followed by 10% N_2 condition, followed by 50% N_2. Higher measurement indicated the presence of more oxidized species in the medium due to the presence of oxygen molecules, low or more negative number indicated fewer oxidized species present. The redox probe was able to show the difference in oxygen availability between 10% and 50% N_2, while the DO probe measured 0% in both cases between 5 to 20 hrs.

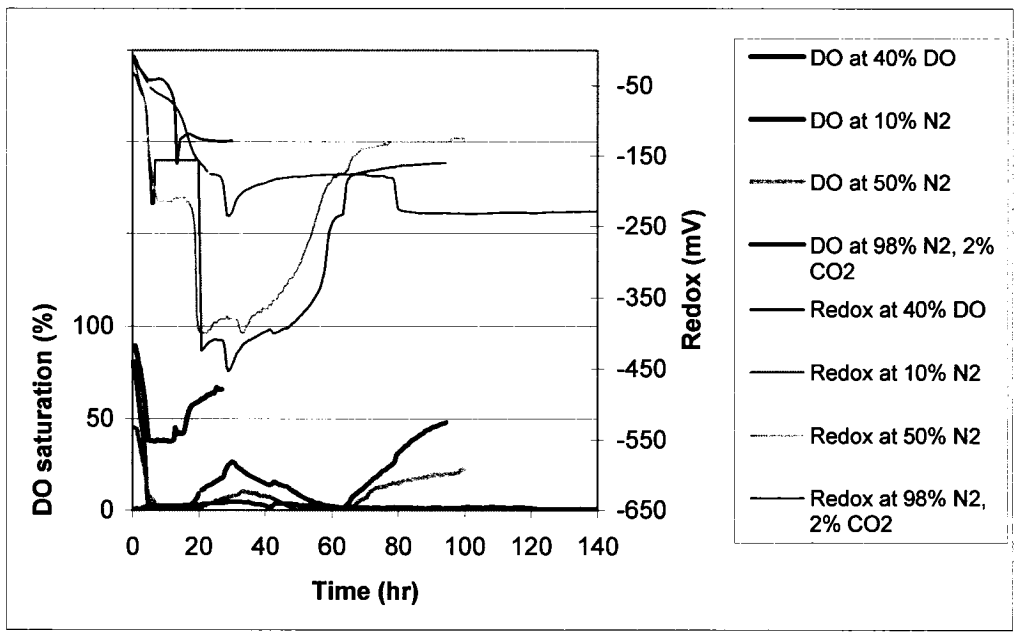

Figure 44. Dissolved oxygen saturation (%) and redox (mV) responses measured during aerobic, microaerobic, and anaerobic cultivations. Redox values normalized to zero mV at 0 hr. DO measurement shown in thick lines, redox measurement shown in fine lines.

On the other hand, DO and redox values rather seemed to oppose each other during mevalonate production phase between 20-60 hrs (Figure 44) for microaerobic and anaerobic cultivations. While the penicillin fermentation was aerobic and hence no mixed acid products influenced the oxidation-reduction potential of the culture, these microaerobic and anaerobic fermentations were full of reduced products (organic acids) that may have impacted the redox potential and overshadowed the measurement of oxygen availability. This was predicted by Dahod [31]: redox probes measure the oxidation state of all species formed in the culture as a result of the biological processes. The highest negative redox value for these microaerobic fermentations corresponded to the highest accumulation of organic acids at 30 hrs. At this time, the DO reading was climbing up slightly due to glucose depletion and reduced cellular respiration. If there were no significant amount of reduced acids in the culture, the redox value may have followed the DO trace. This data suggests that reduced products contributed more than the available oxygen and the oxidized species in the medium to give high negative redox values. After 30 hrs, when cells became accustomed to digesting abundant reduced products as their carbon sources, cell respiration increased shown in decreasing DO saturation until 60 hrs. The corresponding redox measurement during this period showed a positive slope which correlated with the disappearance, or consumption of the organic acids by the cells.

Redox measurement was especially useful during a strict anaerobic cultivation. Because there was no supply of any oxygen, the DO measurement was always zero and gave no additional information about the state of the culture. When the redox probe was

incorporated in the fermentation, it measured differences in cellular activity (Figure 44). At 30 hrs, the lowest minimum redox value was reached when glucose consumption and growth begun. While glucose was consumed between 30-80 hrs, the value became slightly higher indicating oxidized products formed from glucose via glycolysis. After 80 hrs, accumulation of lactate and succinate seemed to reduce the redox measurement under strict anaerobic condition.

In addition to indicating cultivation phases during anaerobic fermentation, redox values were useful in comparing cellular activity from all cultivations. For example, the drop in redox potential correlated well with mevalonate production; the process with the largest drop in the potential (ΔE = -450 mV) corresponded to the highest production of mevalonate and the one with the lowest drop (ΔE = -150 mV) corresponded with the lowest production cultivated at 40% DO.

A redox probe is a tool that gives relative measures of oxygen availability, reduced species, and cellular activity. Its measurements and indications are summarized in Table 11. During the mevalonate fermentation, one needs to consider the formation of reduced products that affects the redox measurement in addition to the oxygen concentration rather than interpreting the redox measurements as oxygen availability.

Table 11. Redox signals and corresponding indications for each category of measurement.

What it measures	Increase in E (positive slope)	Decrease in E (negative slope)	ΔE
O_2 availability	More O_2 available due to low respiration rate	Less O_2 available due to high respiration rate	
Reduced products	Less reduced products present	More reduced products present	
Cellular activity			Big drop in E = increased activity, high mevalonate production anticipated; Low drop in E = low activity, low mevalonate production; No activity when ΔE = zero.

CHAPTER SIX
CONCLUSION AND RECOMMENDATION

Isoprenoids hold great promise as renewable transportation fuels. With approximately 10 billion gallons of ethanol produced between U.S. and Brazil annually (Feb 2007) [47], a market for isoprenoid biofuel compounds that outperform ethanol could be enormous. Microaerobic and anaerobic batch cultivation experiments were performed by varying the rate of oxygen delivery to improve the production of mevalonate and to compare restricted oxygen processes to aerobic processes. The benefits of running microaerobic and anaerobic fermentation as discussed in the literature reviews were demonstrated in the results obtained from this work.

6.1 Aerobic, Microaerobic, and Anaerobic Cultivations of *E. coli* for Heterologous Production of Mevalonate

Aerobic cultivation of the mevalonate producing *E. coli* strain resulted in complete respiratory catabolism of glucose. Although there is no shortage of NAD to breakdown glucose into pyruvate then to acetyl-CoA under aerobic condition, the rate at which acetyl-CoA is taken into TCA cycle seems much faster than the rate of acetyl-CoA incorporation into the mevalonate pathway. The TCA cycle generates CO_2 and the ETC system makes ATPs. As a result, more than 95% of the glucose supply went into producing CO_2 and cell mass as expected. The yield of mevalonate from glucose (wt/wt) was 2-3%. The heterologous production of mevaloante was undesirably low under aerobic cultivation.

The growth of the culture and the production of mevalonate were made possible under strict anaerobic condition with supplementation of CO_2 in the liquid medium. Strict anaerobic and microaerobic conditions successfully controlled the flow of carbon away from biomass generation. However, deficiency in NAD triggered the fermentative catabolism of glucose leading to formation of reduced byproducts, including lactate, succinate, and ethanol for regeneration of NAD, and acetate for ATP production. Formation of these products accounted for more than 70% of the supplied carbon. Once the fermentative products were made, there was no recycling of the products back into the pathways at and above 80% N_2 cultivation conditions. The mevalonate yields from glucose at strict anaerobic condition with CO_2 supplementation was 3% and at low microaerobic conditions were 5-12%. A high degree of anaerobicity was tolerated by *E. coli* strains for the production of recombinant proteins and secondary metabolites.

A desirable operating range of oxygen to nitrogen ratio was narrowed down to high microaerobic range between 65% to 0% N_2 conditions. This could be because this amount of oxygen offered favorable NADH to NAD ratio for the heterologous production of mevalonate. In this range almost all byproducts generated, except for formate and CO_2, were accessible to the mevalonate pathway. The disappearance of these products and additional formation of mevalonate were observed simultaneously over time. A lower percentage of carbon was distributed to CO_2 and cell mass under high microaerobic conditions compared to aerobic cultivation. Furthermore, significant reduction in total organic acids accumulation by the end of the cultivation was seen compared to the low

microaerobic range cultivation. This translated to 35% mevalonate yield from glucose specifically at 65% N_2 condition.

The above findings proved that the hypothesis stated in Section 3.1 holds true: *E. coli* strain harboring a non-native top mevalonate pathway, which does not benefit the cells in generating ATP, was still able to capture high yield by controlling the carbon flow toward the pathway using microaerobic fermentation.

It has been discussed in Chapter 2 that anaerobic cultivations can convert carbon into product more efficiently than aerobic cultivation allowing higher yield of product per substrate. This was not the case for mevaloante. The mevalonate yield per glucose was no better for the anaerobic process than the aerobic process which both yielded ten-fold less compared to the microaerobic process. Similarly, it has been stated that the anaerobic process would be advantageous for the heterologous production of biofuel chemicals. Although the results from this work strongly indicate anaerobic process will not yield profitable conversion, the supply of low oxygen concentration to operate under microaerobic range may still be feasible at scale.

6.2 Recommendation

The carbon recovery data for this work was between 90-110% in most cases. These numbers could be tightened to attain closer to 100% carbon recovery by improving the HPLC method. Some work in method development could achieve better separation of each compound on the column. Similarly, a more sensitive off-gas instrument would help in CO_2 measurements. The CO_2 concentration used in the carbon recovery calculation was solely based on theroretical CO_2 generation for microaerobic and

anaerobic cultivations, instead of the actual measurements in the off-gas. Decreasing the total gas flow rate may also help capture CO_2 measurements from the off-gas analyzer.

In this work, 100% aerobiosis as defined by Alexeeva [21] was inapplicable because 100% air in the inflowing gas was not sufficient to achieve a complete aerobic behavior under batch cultivations. However, Alexeeva's data showed a NADH/NAD ratio that was associated with 100% aerobiosis. Developing a method to obtain information on the NADH/NAD ratio will give us a better understanding of the degree of microaerobicity in the processes described here.

6.3 Future Work

The work here establishes microaerobic fermentation as a good approach for achieving high product yields from carbon substrates. However, significant additional process development will be required in order to implement the technology. Potential follow up experiments include media development, operation under different modes of cultivation, implementation of new tools, and determining the oxygen requirements for different engineered strains or organisms. Once process improvements are made, scale up work will be required to ensure correct oxygen delivery in the production facility.

Batch cultivation with a glucose supply of 30 g/L was investigated in this work. In order to improve mevalonate titer, different glucose delivery and other modes of cultivation could be tested. For instance, using higher glucose concentrations in batch cultivation may help boost mevalonate production from the current titer. This will also help develop an understanding of the organism's tolerance to organic acid build up. On the other hand, organic acid accumulation could be avoided by implementing a fed-batch

process. By feeding glucose at a slow rate, residual glucose concentration in the culture can be maintained close to zero. Simultaneous restriction of oxygen and glucose could eliminate wasteful catabolism of glucose to cell mass and organic acids, yet increase mevalonate production with more glucose addition. A pH stat would be a good candidate for investigation where glucose feed is controlled by the pH of the culture. For that process, the glucose feed would be turned on when pH rises above a set point as the pH change would indicate the disappearance of glucose and acidic byproducts.

Another mode of cultivation worth pursuing is the chemostat. Sustaining the culture in a steady state would allow us to study the real effect of different oxygen delivery on growth and production of mevalonate and byproducts. Following Alexeeva's study, 100% aerobiosis could be defined with the mevalonate producing strain of *E. coli*.

Burke [33] has looked at fermentor system for regulating oxygen at low concentrations with no change in stir or gas flow rate, as briefly discussed in the literature review. Incorporating their computer-controlled system with a three-way valve gas mixer could test conditions between 100% air and 5% DO cultivation conditions which this work did not cover. Using pure oxygen, instead of the mixture of air and nitrogen, with constant stir and flow rate would be another way to test conditions between the two cases.

Evaluation of E (redox) values may improve mevalonate production. An approach for using this parameter for process optimization is described by Shibai [32]. The E value was shown to mirror available oxygen content in the liquid phase in the absence of reduced species [31]. Once a well performing fed-batch process (one that

does not accumulate reduced byproducts) is put in place, oxygen feed may be controlled based on optimal E values.

Application of microaerobic cultivation to different biological systems may show interesting results. Here, heterologous production of mevalonate, a precursor to all isoprenoids, was tested with an *E. coli* strain. This strain could be engineered to lose the ability to make reduced products such as lactate and acetate by knocking out the genes responsible. Such knockout strains have higher specific productivity and/or yield in optimized microaerobic processes. The appropriate oxygen feed rate may vary strain to strain and host to host. Performing the same microaerobic cultivation for the same heterologously expressed product in another host organism may be worthwhile. Above all, a strain that contains a full isoprenoid pathway will be more relevant for the production of biofuels.

It has been reported that the rate of oxygen transfer from the gaseous to the liquid phase changes with scale due to a difference in geometry and mixing efficiency varying the volumetric mass transfer coefficient, K_La [21]. This work showed a wide range of acceptable oxygen delivery rate for the optimal heterologous production of mevalonate, which will help with process scale up. Once the process has been developed further, work can be undertaken first at the pilot scale and then at the production scale to implement a fuel's fermentation.

REFERENCES

1. Wikipedia. "Biofuels." Retrieved 20 February 2007, from http://en.wikipedia.org/wiki/Biofuel

2. EIA. "Annual Energy Outlook 2003 with Projections to 2025." Retrieved 22 February 2007, from http://www.eia.doe.gov/bookshelf/brochures/aeo2003/AEOBrochure.html

3. A. Scott and M. Bryner, "*Alternative fuels: Rolling out next-generation technologies*," Chemical Week, **168(43)**, 4 (2006).

4. B. Stambuk (2007). Fuel ethanol production in Brazil: challenges and opportunities for yeast.

5. N.N. Nichols, B.S. Dien, R.J. Bothast and M.A. Cotta (2006). The corn ethanol industry. Alcoholic Fuels. S. Minteer. Boca Raton, FL, CRS Press.: 59-78.

6. M.L. Shuler and F. Kargi, Bioprocess Engineering Basic Concepts, 2nd ed. (Prentice-Hall, Inc., Upper Saddle River, New Jersey, 2002).

7. R. Rapier. (2006, 1 May 2006). "Bio-Butanol." Retrieved 29 March 2007, from http://i-r-squared.blogspot.com/2006/05/bio-butanol.html

8. ScienceDaily. (12 February 2007). "MIT experts foresee efficient ethanol production." Retrieved 20 February 2007, from http://www.sciencedaily.com/releases/2007/02/070210170439.htm

9. H.P. Blaschek (2007). "*The acetone, butanol, ethanol fermentation and the road to commercialization*," Society for Industrial Microbiology Annual Meeting, Denver, CO.

10. Wikipedia. (14 March 2007). "Metabolic engineering." Retrieved 14 April 2007, from http://en.wikipedia.org/wiki/Metabolic_engineering

11. B.N. Mijts and C. Schmidt-Dannert, "*Engineering of secondary metabolite pathways*," Curr Opin Biotechnol, **14(6)**, 597-602 (2003).

12. P.I. Nikel, M.J. Pettinari, M.A. Galvagno and B.S. Mendez, "*Poly(3-hydroxybutyrate) synthesis by recombinant Escherichia coli arcA mutants in microaerobiosis*," Applied and Environmental Microbiology, **72(4)**, 2614-2620 (2006).

13. V.J. Martin, D.J. Pitera, S.T. Withers, J.D. Newman and J.D. Keasling, "*Engineering a mevalonate pathway in Escherichia coli for production of terpenoids*," Nat Biotechnol, **21(7)**, 796-802 (2003).

14. Y. Zhu, M.A. Eiteman, K. DeWitt and E. Altman, "*Homolactate fermentation by metabolically engineered Escherichia coli strains*," Appl Environ Microbiol, **73(2)**, 456-64 (2007).

15. J. Lau, C. Tran, P. Licari and J. Galazzo, "*Development of a high cell-density fed-batch bioprocess for the heterologous production of 6-deoxyerythronolide B in Escherichia coli*," J Biotechnol, **110(1)**, 95-103 (2004).

16. J. Maury, M.A. Asadollahi, K. Moller, A. Clark and J. Nielsen, "*Microbial isoprenoid production: an example of green chemistry through metabolic engineering*," Adv Biochem Eng Biotechnol, **100**, 19-51 (2005).

17. H. Lin, G.N. Bennett and K.Y. San, "*Fed-batch culture of a metabolically engineered Escherichia coli strain designed for high-level succinate production and yield under aerobic conditions*," Biotechnol Bioeng, **90(6)**, 775-9 (2005).

18. H.G. Lawford and J.D. Rousseau, "*Effect of oxygen on ethanol production by a recombinant ethanologenic E. coli*," Appl Biochem Biotechnol, **45-46**, 349-66 (1994).

19. S.Y. Lee, "*High cell-density culture of Escherichia coli*," Trends in Biotechnology, **14(3)**, 98-105 (1996).

20. S. Fink. "Coenzyme Q10 and prevention of Parkinsons's disease." Retrieved 31 August 2007, from http://altmed.creighton.edu/Parkinsons/cq10.htm

21. S. Alexeeva, B. de Kort, G. Sawers, K.J. Hellingwerf and M.J.T. de Mattos, "*Effects of limited aeration and of the ArcAB system on intermediary pyruvate catabolism in Escherichia coli*," Journal of Bacteriology, **182(17)**, 4934-4940 (2000).

22. B.M. Bakker, K.M. Overkamp, A.J.A. van Maris, P. Kotter, M.A.H. Luttik, J.P. van Dijken and J.T. Pronk, "*Stoichiometry and compartmentation of NADH metabolism in Saccharomyces cerevisiae*," Fems Microbiology Reviews, **25(1)**, 15-37 (2001).

23. S. Becker, G. Holighaus, T. Gabrielczyk and G. Unden, "*O-2 as the regulatory signal for FNR-dependent gene regulation in Escherichia coli*," Journal of Bacteriology, **178(15)**, 4515-4521 (1996).

24. L.L. Bermejo, N.E. Welker and E.T. Papoutsakis, "*Expression of Clostridium acetobutylicum ATCC 824 genes in Escherichia coli for acetone production and acetate detoxification*," Applied and Environmental Microbiology, **64(3)**, 1079-1085 (1998).

25. R. Carlson, A. Wlaschin and F. Srienc, "*Kinetic studies and biochemical pathway analysis of anaerobic poly-(R)-3-hydroxybutyric acid synthesis in Escherichia coli*," Applied and Environmental Microbiology, **71(2)**, 713-720 (2005).

26. R.J. van Wegen, S.Y. Lee and A.P.J. Middelberg, "*Metabolic and kinetic analysis of poly(3-hydroxybutyrate) production by recombinant Escherichia coli*," Biotechnology and Bioengineering, **74(1)**, 70-80 (2001).

27. K.K. Cheng, D.H. Liu, Y. Sun and W.B. Liu, "*1,3-propanediol production by Klebsiella pneumoniae under different aeration strategies*," Biotechnology Letters, **26(11)**, 911-915 (2004).

28. A.E. Wheals, L.C. Basso, D.M. Alves and H.V. Amorim, "*Fuel ethanol after 25 years*," Trends Biotechnol, **17(12)**, 482-7 (1999).

29. F.L. Wang and S.Y. Lee, "*Production of poly(3-hydroxybutyrate) by fed-batch culture of filamentation-suppressed recombinant Escherichia coli*," Applied and Environmental Microbiology, **63(12)**, 4765-4769 (1997).

30. S. Becker, D. Vlad, S. Schuster, P. Pfeiffer and G. Unden, "*Regulatory O-2 tensions for the synthesis of fermentation products in Escherichia coli and relation to aerobic respiration*," Archives of Microbiology, **168(4)**, 290-296 (1997).

31. S.K. Dahod, "*Redox potential as a better substitute for dissolved oxygen in fermentation process control*," Biotechnol Bioeng, **24(9)**, 2123-2125 (1982).

32. H. Shibai, A. Ishizaki, K. Kobayashi and Y. Hirose, "*Simultaneous measurement of dissolved oxygen and oxidation-reduction potentials in the aerobic culture*," Agr. Biolo. Chem., **38(12)**, 2407-2411 (1974).

33. P.V. Burke, K.E. Kwast, F. Everts and R.O. Poyton, "*A fermenter system for regulating oxygen at low concentrations in cultures of Saccharomyces cerevisiae*," Applied and Environmental Microbiology, **64(3)**, 1040-1044 (1998).

34. A. De Leon, V. Hernandez, E. Galindo and O.T. Ramirez, "*Effects of dissolved oxygen tension on the production of recombinant penicillin acylase in Escherichia coli*," Enzyme and Microbial Technology, **33(5)**, 689-697 (2003).

35. E.A. Sandoval-Basurto, G. Gosset, F. Bolivar and O.T. Ramirez, "*Culture of Escherichia coli under dissoved oxygen gradients simulated in a two-compartment scale-down system: metabolic response and production of recombinant protein*," Biotechnol Bioeng, **89(4)**, 453-463 (2004).

36. M.G. Wiebe, E. Rintala, A. Tamminen, H. Simolin, L. Salusjarvi, M. Toivari, J.T. Kokkonen, J. Kiuru, R.A. Ketola, P. Jouhten, A. Huuskonen, H. Maaheimo, L. Ruohonen and M. Penttila, "*Central carbon metabolism of Saccharomyces cerevisiae in anaerobic, oxygen-limited and fully aerobic steady-state conditions and following a shift to anaerobic conditions*," FEMS Yeast Res, (2007).

37. S. Alfenore, X. Cameleyre, L. Benbadis, C. Bideaux, J.L. Uribelarrea, G. Goma, C. Molina-Jouve and S.E. Guillouet, "*Aeration strategy: a need for very high ethanol performance in Saccharomyces cerevisiae fed-batch process*," Appl Microbiol Biotechnol, **63(5)**, 537-42 (2004).

38. D.J. Korz, U. Rinas, K. Hellmuth, E.A. Sanders and W.D. Deckwer, "*Simple fed-batch technique for high cell density cultivation of Escherichia coli*," J Biotechnol, **39(1)**, 59-65 (1995).

39. J. Chen, A.L. Tannahill and M.L. Shuler, "*Design of a system for the control of low dissolved oxygen concentrations: critical oxygen concentrations for Azotobacter vinelandii and Escherichia coli*," Biotechnol Bioeng, **27(2)**, 151-5 (1985).

40. Dionex. (2005). "IonPac ICE-AS6 Manual." Retrieved 2 May 2007, from http://www1.dionex.com/en-us/webdocs/4453_34961-07_ICE_AS6_Manual_V26.pdf

41. NovaBiomedical. Retrieved 30 April, 2007, from http://www.novabiomedical.com/bioprofile/bpanalyzers.html#measuretech

42. Sartorius, MFCS/win Operating Manual Version 2.1, (Melsungen, 2003).

43. A.D. Frey, J. Fiaux, T. Szyperski, K. Wuthrich, J.E. Bailey and P.T. Kallio, "*Dissection of central carbon metabolism of hemoglobin-expressing Escherichia coli by 13C nuclear magnetic resonance flux distribution analysis in microaerobic bioprocesses*," Appl Environ Microbiol, **67(2)**, 680-7 (2001).

44. BioCyc. "*E. coli* K-12 pathway: mixed fermentation pathway." Retrieved 31 August 2007, from http://biocyc.org/ECOLI/NEW-IMAGE?type=PATHWAY&object=FERMENTATION-PWY&detail-level=2

45. K. McGrath and D. Kaplan, Protein-Based Materials, 1st ed. (Birkhauser, Boston, 1997).

46. M. Beals, L. Gross and S. Harrel. (1999). "Metabolism for energy and the respiratory quotient." Retrieved 24 August 2007, from http://www.tiem.utk.edu/~gross/bioed/webmodules/respiratoryquotient.html

47. J.R. Mielenz (2007). "*Advanced strategies for biomass ethanol production,*" Society for Industrial Microbiology Annual Meeting, Denver, CO.

APPENDIX
ABBREVIATION AND ACRONYMS

Abbreviation	**Acronym**	**Units**
1,3 PD	1,3-propanediol	
AMP	adenosine monophosphate	
atoB	acetoacetyl-CoA thiolase	
ATP	adenosine triphosphate	
CER	carbon dioxide evolution	mmol/L/min
CO_2	carbon dioxide	
CoA	coenzyme A	
DAP	data acquisition processor	
DCW	dry cell weight	g/L
DMAPP	dimethylallyl diphosphate	
DO	dissolved oxygen	%
DOC	dissolved oxygen concentration	%
DOT	dissolved oxygen tension	%
E	redox potential	mV
EtOH	ethanol	
ETS chain	electron transport system chain	
FPP	farnesyl diphosphate	
GMP	good manufacturing practice	
HMGS	hydroxymethylglutaryl-CoA synthase	
HPLC	high performance liquid chromatography	
IPP	isopentenyl diphosphate	
IPTG	isopropyl B-D-1-thiglactopyranoside	
K_La	volumetric mass transfer coefficient	hr^{-1}
K_m	Michaelis-Menten constant	
LDH	lactate dehydrogenase	
MFCS	mass flow control system	
MTBE	methyl tert-butyl ether	
N_2	nitrogen gas	
NAD (NAD+)	nicotinamide adenine dinucleotide	
NADH	nicotinamide adenine dinucleotide, reduced form	
NADP	nicotinamide adenine dinucleotide phosphate	
NADPH	nicotinamide adenine dinucleotide phosphate, reduced form	
O_2	oxygen gas	
OD_{600}	optical density at 600nm	
OUR	oxygen uptake rate	mmol/L/min
PEP	phosphoenolpyruvate	

PFL	pyruvate formate lyase	
PHA	polyhydroxyalkanoate	
PHB	poly(3-hydroxybutyrate)	
P_i	inorganic phosphate	
PID	proportional-integral-differential	
pO_2	partial oxygen	%
PSDVB	Poly(styrene-divinylbenzene)	
qO_2	specific rate of respiration	mmol/g DCW/hr
RI	refractory index	
TCA	tricarboxylic acid	
tHMGR	trancated hydroxymethylglutaryl-CoA reductase	
TM	trace metal	
vvm	Volume gas/volume liquid/min	
$Y_{P/S}$	product yield on substrate	
$Y_{P/X}$	product yield on biomass	
$Y_{X/S}$	biomass yield on substrate	